

Physical exercise rescues defective neural stem cells and neurogenesis in the adult subventricular zone of Btg1 knockout mice

Valentina Mastrorilli^{1,7} · Chiara Scopa^{2,3} · Daniele Saraulli^{1,5} · Marco Costanzi^{1,5} · Raffaella Scardigli^{3,4} · Jean-Pierre Rouault⁶ · Stefano Farioli-Vecchioli¹ · Felice Tirone¹ 

Received: 9 November 2016 / Accepted: 23 January 2017
© Springer-Verlag Berlin Heidelberg 2017

Abstract Adult neurogenesis occurs throughout life in the dentate gyrus (DG) and the subventricular zone (SVZ), where glia-like stem cells generate new neurons. Voluntary running is a powerful neurogenic stimulus triggering the proliferation of progenitor cells in the DG but, apparently, not in the SVZ. The antiproliferative gene Btg1 maintains the quiescence of DG and SVZ stem cells. Its ablation causes intense proliferation of DG and SVZ stem/progenitor cells in young mice, followed, during adulthood, by progressive decrease of the proliferative capacity. We have previously observed that running can rescue the deficit of

DG Btg1-null neurogenesis. Here, we show that in adult Btg1-null SVZ stem and neuroblast cells, the reduction of proliferation is associated with a longer cell cycle and a more frequent entry into quiescence. Notably, running increases proliferation in Btg1-null SVZ stem cells highly above the levels of sedentary wild-type mice and restores normal values of cell cycle length and quiescence in stem and neuroblast cells, without affecting wild-type cells. Btg1-null SVZ neuroblasts show also increased migration throughout the rostral migratory stream and a deficiency of differentiated neurons in the olfactory bulb, possibly a consequence of premature exit from the cycle; running, however, normalizes migration and differentiation, increasing newborn neurons recruited to the olfactory circuitry. Furthermore, running increases the self-renewal of Btg1-null SVZ-derived neurospheres and, remarkably, in aged Btg1-null mice almost doubles the proliferating SVZ stem cells. Altogether, this reveals that SVZ stem cells are endowed with a hidden supply of self-renewal capacity, coupled to cell cycle acceleration and emerging after ablation of the quiescence-maintaining Btg1 gene and following exercise.

Stefano Farioli-Vecchioli and Felice Tirone contributed equally.

Electronic supplementary material The online version of this article (doi:10.1007/s00429-017-1376-4) contains supplementary material, which is available to authorized users.

✉ Stefano Farioli-Vecchioli
stefano.fariolivecchioli@cnr.it

✉ Felice Tirone
felice.tirone@cnr.it

¹ Institute of Cell Biology and Neurobiology, National Research Council, Fondazione Santa Lucia, via del Fosso di Fiorano 64, 00143 Rome, Italy

² University Roma 3, Rome, Italy

³ European Brain Research Institute (EBRI), Rome, Italy

⁴ Institute of Translational Pharmacology, National Research Council, Rome, Italy

⁵ Department of Human Sciences, LUMSA University, Rome, Italy

⁶ Centre Léon Bérard-Université Claude Bernard Lyon I, Lyon, France

⁷ Dipartimento di Biologia e Biotecnologie Charles Darwin, Sapienza Università di Roma, Rome, Italy

Keywords Running · Adult neurogenesis · Neural stem/progenitor cells · Cell cycle kinetics · Proliferation · Differentiation

Introduction

A growing number of preventive/therapeutic approaches in the field of stem cell research are aimed at harnessing endogenous neurogenesis, in attempts to partially replace neuron depletion as a result of neurodegenerative disease, brain damage, or aging. In the last few years, in this context, running, and more generally physical activity, has

received particular attention as a potential brain health method able to elevate human cognitive function and to improve brain functioning throughout the life span. By affecting abnormal protein deposition, increasing neurotrophic factors (such as BDNF and IGF-1), improving cerebral blood flow, and decreasing systemic inflammation, it has been shown that physical exercise may protect against degenerative brain changes (Intlekofer et al. 2013). Moreover, many observations suggest that physical activity highly reduces the risk of several diseases by counteracting the onset of cardiovascular insults, stroke, and obesity-related diseases (Chodzko-Zajko et al. 2009).

Interest in adult neurogenesis has grown in recent years, because a large number of pre-clinical studies have well-correlated mental and neurological disorders, such as drug abuse, major mood disorders, and neurodegenerative diseases, with change in the degree of adult neurogenesis (Dimitrov et al. 2014; Danzer et al. 2012; Ruan et al. 2014). At the same time, a growing body of evidence has established that running positively affects learning and memory, induces partial recovery from traumatic brain injury, exerts a preventive effect on stress/depression disorders, and, finally, improves hippocampal adult neurogenesis (van Praag et al. 2008; Itoh et al. 2011; Brown et al. 2003).

In animal models, it is clearly demonstrated that voluntary physical exercise positively modulates hippocampal adult neurogenesis eliciting a potent pro-neurogenic and pro-cognitive effect (Ryan and Kelly 2016). It has been shown that voluntary running, in fact, affects many aspects of hippocampal adult neurogenesis, such as proliferation, differentiation, and functional integration in the hippocampal network (Farioli-Vecchioli and Tirone 2015). In contrast, forced physical activity, such as water-maze learning or yoked swimming, seems not able to increase the number of surviving newborn cells in the dentate gyrus (van Praag et al. 1999).

The pro-neurogenic effect exerted by physical activity is strictly dependent on increased proliferation of hippocampal progenitors, which results in a rise of the number of the early post-mitotic neurons (Kronenberg et al. 2006). There are several hypotheses trying to ascertain the running-induced enhancement of hippocampal neural precursor cells, as exhaustively reviewed by Overall et al. 2016. Among the putative mechanisms, a recent study has highlighted the role of cell cycle kinetic, and in particular of S-phase length, in the running-dependent increase of hippocampal progenitor proliferation (Farioli Vecchioli et al. 2014; Farioli-Vecchioli and Tirone 2015). The enhanced proliferation of hippocampal newly generated neurons is strictly associated with changes in neuronal morphology (increased spine density and dendritic arborisation), hippocampal plasticity, and long-term potentiation (Dietrich et al. 2008; Lin et al. 2012; Stranahan et al. 2009).

The relationship among physical activity adult neurogenesis and memory functions has been explored also during normal aging. Physical exercise has been shown to protect against the loss of neuroplasticity and age-related cell proliferation decline. For example, in adult mice, the running wheel exerted for 1 month is able to increase the survival of newborn cells and consequently to improve spatial memory in Morris water mazes (van Praag et al. 2005). Running is also able to act as protective factor during cognitive decline and to counteract the onset of dementia, as shown by a recent research indicating that prolonged voluntary physical exercise is able to induce hippocampal neurogenesis in a mouse model of Alzheimer's disease, reducing hippocampal spatial-memory loss (Paillard et al. 2015).

Surprisingly, recent data have shown that exercise is able to induce neurogenesis in the hypothalamus and ependymal lining of the third ventricle, leading to recovery of homeostatic functions in the adult brain after brain injury (Niwa et al. 2016). Although the running-dependent enhancement of hippocampal neurogenesis is a well-established phenomenon, the subventricular zone (SVZ), which represents the other main neurogenic niche in the murine adult brain (Alvarez-Buylla et al. 2008), seems not respond to exercise (Brown et al. 2003), although this issue remains still debated (Bednarczyk et al. 2009). Indeed, a recent paper demonstrates that the number of SVZ-derived neurospheres rises with voluntary running in aged mice (Blackmore et al. 2012) and another evidence suggests a running-dependent recovery of altered SVZ neurogenesis following chronic infusion of corticosterone (Lee et al. 2016).

The SVZ is the largest germinal region in the adult mammalian brain. The primary source of new neurons in this neurogenic niche arises from a subpopulation of slowly dividing astrocyte-like neural stem cells, termed type B cells, adjacent to a layer of ependymal cells (Doetsch et al. 1999; Laywell et al. 2009; Imura et al. 2003). Type B cells produce type C cells, a type of transient-amplifying cell that divides rapidly to produce young neurons, also known as neuroblast or type A cells. In the anterior SVZ, neuroblasts, once exited from the cell cycle, migrate as a chain along the rostral migratory stream (RMS) in the olfactory bulb (Lim and Alvarez-Buylla 2016). The rostral extension of the RMS forms the core of the OB, through which the young neurons enter in the mouse OB and complete their tangential trajectory. Upon entering the bulb through its core, the young neurons migrate radially into the granule and glomerular layer where they terminally differentiate into granular and periglomerular local GABAergic inhibitory interneurons (Kosaka et al. 1995; Carleton et al. 2003; Kohwi et al. 2005). It has been shown that SVZ neurogenesis is positively regulated by the olfactory experience: deprivation of olfactory sensory inputs delays maturation and survival of newborn neurons in the OB. More specifically,

sensory experience and the activity of young neurons are critical for the survival of 14- to 28-day-old neurons. On the other hand, enriched odor exposure increases the survival of newborn neurons and transiently improves odor memory, suggesting a role for SVZ neurogenesis in this memory process (Zhao et al. 2008). To ensure a continuous supply of adult-born interneurons to the OB, a fine spatio-temporal tuning of the different steps of SVZ neurogenesis must be guaranteed.

In this study, we have analyzed the effect of physical exercise in orchestrating the different steps of subventricular neurogenesis in a mouse model lacking the anti-proliferative gene *Btg1*, which displays an impaired subventricular neurogenesis (Farioli Vecchioli et al. 2014). *Btg1* loss-of-function mice exhibit a strong reduction of proliferation, partly due to the S-phase lengthening, associated with a premature cell cycle exit and an anticipated migration of neuroblasts toward the OB, where the cells fail to fully differentiate and consequently to be specifically recruited into olfactory-dependent memory circuitry. We show that 12 days of voluntary running are able to totally revert the impaired SVZ neurogenesis in the *Btg1* knock out mouse, mainly through a dramatic cell cycle shortening-dependent expansion of type B cells, which, in turn, induces a re-establishment of the physiological neurogenic progression of the SVZ newborn neurons and an improvement of their maturation, survival, and functional activation.

Materials and methods

Animals

C57BL/6 *Btg1* KO mice had been generated previously (Farioli-Vecchioli et al. 2012). Genotyping from tail samples was performed as elsewhere described (Farioli-Vecchioli et al. 2012). Mice were housed under a 12-h light/12-h dark cycle at a constant temperature of 21 °C provided with food and water *ad libitum*. At 2 months of age, they were randomly assigned to running wheel or standard cages for 5 and 12 days. Exercise duration was defined in consideration of the previous data obtained in the analysis of the dentate gyrus of *Btg1* KO mice after running (Farioli-Vecchioli et al. 2014). Distance runs were recorded daily with an automatic counter. After 5 and 12 days, mice were subjected to perfusion or were put back in standard cages to be sacrificed at different times from the end of the run. Animals were treated following the Italian Ministry of Health and directive 2010/63/EU guidelines.

Immunohistochemistry

Brains were collected after transcardiac perfusion with 4% paraformaldehyde (PFA) in phosphate-buffered saline (PBS) and kept overnight in PFA. Afterwards, brains were equilibrated in sucrose 30% and cryopreserved at -80°C . Brains were embedded in *Tissue-Tek OCT* (Sakura Finetek, Torrance, CA) and cut with a cryostat at -25°C throughout the whole rostrocaudal extent of the SVZ in one-in-six series of 40 μm free-floating coronal section (240 μm apart). Histological sections were put in sodium azide (NaN_3) 0.03% PBS at 4 °C for short-term storage, or in anti-freezing solution (30% glycerol and 30% ethylene glycol in PBS) for long-term preservation at -20°C . Sections were stained for multiple labeling using fluorescent methods. After a single wash with glycine for 10 min, sections were permeabilized with 0.3% Triton X-100 in PBS for 10 min. Thereafter, sections were incubated in a blocking solution containing 3% normal donkey serum (NDS) in 0.3% Triton X-100 in PBS for an hour to saturate the aspecific sites and then they were incubated in a blocking solution containing primary antibodies for 16–18 h at 4 °C. Primary antibodies used were a mouse monoclonal antibodies raised against Nestin (Chemicon International; MAB353; 1:150), NeuN (Chemicon International; MAB353; 1:300), or against pHH3 (Cell Signaling Technology, Danvers, USA; 9706; 1:100); a rabbit monoclonal antibody was used against Ki67 (LabVision Corporation, Fremont, USA; SP6; 1:150); rabbit polyclonal antibodies against cleaved (activated) Caspase-3 (Cell Signaling Technology, Santa Cruz, USA; 9661; 1:100), c-fos (Cell Signaling) or goat polyclonal antibodies against GFAP (Santa Cruz Biotechnology; Sc-6170; 1:300), or DCX (Santa Cruz Biotechnology; Sc-8066; 1:300). To visualize the primary antibody binding, donkey secondary antibodies were used conjugated to Cy2 (Jackson ImmunoResearch, West Grove, USA; 1:200 in PBS) or TRITC (tetramethylrhodamine isothiocyanate; Jackson ImmunoResearch, West Grove, PA, USA; 1:300 in PBS), or donkey secondary antibodies conjugated to Alexa 647 (Invitrogen, San Diego, CA, USA; 1:300 in PBS). Nuclei were observed incubating sections with Hoechst (1:500).

Cell numbers in the SVZ and in the OB were obtained with stereological analysis, by counting cells expressing the indicated marker, visualized with confocal microscopy throughout the whole rostrocaudal extent of these structures in one-in-ten series of 40- μm free-floating serial coronal section (240 μm apart). Cell numbers obtained for each SVZ and olfactory bulb section were divided for the corresponding area of the section, as described (Colak et al. 2008), to obtain the average number of SVZ or olfactory bulb cells per square millimeter. Areas were obtained by tracing the outline of the whole SVZ, or olfactory bulb, identified by the presence of cell nuclei stained by Hoechst

33,258 on a digital picture captured and measured using the I.A.S. software (Delta Sistemi, Rome, Italy). The volumes of the SVZ were calculated, multiplying the average SVZ area by section thickness and by number of sections (one-in-ten series of 40- μ m coronal sections). The running animals number were placed in pairs in cages with wheels. 3-to-6 male mice per condition were analyzed (running or not running). The I.A.S. software was also used to count labeled cells.

BrdU treatments and thymidine analogs detection

To calculate the cell cycle exit precisely, 2-month-old animals were treated with a single injection of bromodeoxyuridine (BrdU, i.p. 95 mg/kg) and perfused 48 h afterwards. SVZ neurons migrating in the rostral migratory stream (RMS) were detected by treating P60 mice with 5-daily injections of BrdU (95 mg/kg i.p.), followed by perfusion 6 days after the last injection (P71). In addition, 28-day-old neurons present in the OB after migration from the SVZ were detected after treatment with five daily injections of BrdU (95 mg/kg i.p.) from P60 to P64 followed by olfactory stimulation 4 weeks later.

To perform BrdU detection, DNA was denatured with 2N HCl for 40 min at 37°C to facilitate antibody access, followed by 0.1 M borate buffer pH 8.5 for 20 min. Sections were incubated overnight at 4°C with a primary antibody rat anti-BrdU (Serotech, Raleigh, USA; MCA2060) diluted in TBS containing 0.1% Triton, 0.1% Tween, and 3% normal donkey serum (blocking solution).

Immunohistochemistry against CldU and IdU was carried out using more stringent conditions to minimize any possible crossreactivity of the antibodies. The incubation with HCl 2N was reduced to 10 min and the NDS was used at 5%. After the HCl administration, as well as after the incubation in primary antibodies, the sections were washed five times with TBS. Detection of halogenated thymidine analogs was performed using anti-BrdU (DB Biosciences, San Jose, USA; BD 44) for IdU and rat anti-BrdU (Serotech, Raleigh, USA; MCA2060) for CldU. Antibody specificity was analyzed in mice that were injected with either IdU or CldU only.

Cell cycle analysis

To determine the precise length of S-phase (T_s) and total cell cycle (T_c), we adopted a new method developed by Brandt et al. (2012) which requires the administration of two halogenated thymidine analogs, CldU (5-chlorodeoxyuridine) and IdU (5-iodo-2-deoxyuridine). Two-month-old Btg1 knockout and wild-type mice received a single i.p. injection of 57.5 mg/kg IdU in 0.2 N NaOH 0.9% NaCl solution, followed by a single i.p. injection of 42.5 mg/kg

CldU in sterile 0.9% NaCl solution and 45 min after the last injection animals were sacrificed. Immunohistochemistry allowed detection and quantification of the number of cells that incorporated IdU, CldU, or both of them.

To precisely calculate the T_s length, adult mice received an IdU injection 3 h prior to a CldU-injection and were sacrificed 45 min later: a 3-h interinjection interval between the two analogs gave rise to three different cell population (Fig. 5.1): CldU⁺/IdU⁻ cells (green) that entered S-phase of cell cycle during the 3-h interval, IdU⁺/CldU⁻ cells (blue) that left S-phase between the two injections and IdU⁺/CldU⁺ double-labeled cells (cyan) that were in S-phase during both injections.

According to the equation developed by the authors, the ratio among IdU⁺/CldU⁻ cells (a) and the total number of IdU⁺ cells ($a + b$) is equal to the ratio among 3 h (interinjection interval) and T_s . Similarly, to determine the total cell cycle length (T_c), we chose a 16-h interval between the two injections preventing labeling the same S-phase twice: the ratio among the cells that entered the S-phase during the interinjection interval (CldU⁺/IdU⁻) and the total CldU⁺ cells is equal to the ratio among y and T_s .

Thereafter, we estimated the duration of the phase G2 + M using the percentage of labeled mitoses method (Cai et al. 1997; Beukelaers et al. 2011) by injecting a single pulse of BrdU, (i.p. 95 mg/kg in saline) and perfusing them 1, 2, 2.5, 3, 4, or 5 h later. Immunohistochemistry was performed against BrdU and PH3 (phosphohistone 3, a marker of mitotic cells). The time elapsed between the BrdU injection and the moment when all the labeled cells became positive for PH3 corresponds to G2 + M.

Finally, we determined the G1 length by subtracting the length of cell cycle phases calculated to the total cell cycle length.

Olfactory stimulation

To investigate the effects of physical exercise on the recruitment of OB newborn neurons, mice underwent olfactory stimulation. In a cage identical to those normally used to house the animals, with the floor covered by a thin layer of wood chip bedding, filter paper soaked with octanal diluted in mineral oil (25 μ l) was placed in close proximity to one side of the cage. During five successive sessions, lasting 5 min each and followed by 5-min interval, each mouse was exposed to the filter paper. To quantify the number of newborn neurons activated, mice were sacrificed 90 min after the last stimulation, and the number of new neurons activated was measured by concomitant positivity to BrdU, NeuN, and immediate early gene (IEG) c-fos.

In vitro analysis

Btg1-null or wild-type 2-month-old mice were euthanized by CO₂, followed by cervical dislocation and the brains were successively removed. SVZ were dissected out as described before (Farioli-Vecchioli et al. 2012) and cells were isolated by enzymatic digestion (1.33 mg/ml trypsin, 0.7 mg/ml hyaluronidase, and 0.2 mg/ml kynurenic acid) for 30 min at 37 °C pipetting every 15 min with a small-bore Pasteur pipette allowing mechanical dissociation. In every tube, 5 ml of DMEM/F12 was added to consent tissues precipitation: after 10 min at room temperature, the superior phase was removed, leaving a small volume on the tip of the tube. Then, samples were centrifuged at 200 g for 5 min, supernatant was removed, and the pellet was pipetted 40–50 times to fully dissociate cells. Neurospheres were grown in a humidified incubator at 37 °C in 5% CO₂ and cultured in DMEM/F12 medium supplemented with B27 and EGF (20 ng/ml) and bFGF (10 ng/ml). Cells were passaged every 7th day by mechanically dissociating neurospheres into single cells.

To perform a neurosphere assay, cells isolated from SVZ were cultured under clonal conditions, in which neurospheres are generated from single cells and serving as an index of the number of in vivo neural stem cells. Cells were plated at 10 cells/μl in 24-well (0.5 ml/well) uncoated plates in growth medium. The total number of neurospheres was counted after 7 days in vitro (7 DIV).

To evaluate expansion capacity, primary neurospheres were dissociated into single cells and plated at the same clonal density. The number of clonal neurospheres was counted for each condition. Then, primary neurospheres were dissociated and plated at the same density. We measured their size, which was expressed as a volume calculated after measuring their diameter in phase contrast pictures (assuming a spherical shape). Then, secondary neurospheres were dissociated and the number of cells was determined and expressed as average expansion from the initial starting population (number of cells from secondary neurospheres at 7 DIV/number of seeded cells).

For the growth curve, 8000 cells from wild-type and knockout neurospheres at passage 5 were seeded in 24-well plates. At each subculture passage (every 7 days), the viable cells were counted and totally re-plated under the same conditions.

Explant cultures

Brains were dissected and placed in ice in Hank's balanced salt solution (HBSS), and cut in coronal slices. Under the stereomicroscope, slices were cut in pieces of 50–200 μm of diameter, which were then resuspended in Neurobasal A medium (Invitrogen) mixed 1:3 with Matrigel (BD

Biosciences). The tissue pieces embedded in Matrigel were then plated onto 24-well dishes (BD Biosciences, NJ, USA) on ice, and then left for 10 min at 37 °C to allow polymerization. The explants thus obtained were cultured in Neurobasal A medium supplemented with B27, Glutamax, and a penicillin–streptomycin mixture (Invitrogen) at 37 °C in humidified air containing 5% CO₂. At the end of the experiments, the explants were fixed in 4% PFA for 20 min, washed in PBS and analyzed with an inverted microscope (Leica DMIRB). The migration was quantified by measuring the area of the bright cellular region around an explant, normalized to the explant perimeter.

Statistical analysis

Statistical analyses were performed using two-way ANOVA (genotype x treatment) for comparing the effects of running in WT and KO mice. Whenever appropriate, post-hoc comparison were performed by Fisher's protected least significant difference (PLSD) test. All experimental groups were composed of at least four animals. Differences were considered statistically significant at $p < 0.05$. All data were expressed as mean values \pm SEM.

Results

12 days of running induce a large increase of proliferation of stem and progenitor cells in the SVZ of Btg1 ko mice

To analyze the effect of voluntary physical exercise on the defective neurogenesis in the subventricular zone (SVZ) of the Btg1 knockout mice, we put Btg1 wild-type and knockout mice in cages with free access to a running wheel for 12 days. As previously reported, we did not detect any difference in the distance run between Btg1 wt and ko mice (data not shown; see Farioli-Vecchioli et al. 2014). First, we measured the proliferation rate of progenitor cells and neuroblasts after running in the SVZ of the mice groups under study: sedentary Btg1 wt mice (WT NO RUN), exercised Btg1 wt mice (WT RUN), sedentary Btg1 knockout mice (KO NO RUN), and exercised Btg1 knockout mice (KO RUN). Our recent data clearly demonstrated that in the KO mice, physical exercise totally recovered the declined proliferation observed in the sedentary KO mice and triggered the overproduction of proliferating type B (identified as Ki67⁺GFAP⁺) and type A cells (identified as KI67⁺DCX⁺) (Farioli-Vecchioli et al. 2014).

Then, we asked whether the increased neurogenesis observed in the SVZ of KO RUN mice was strictly dependent on the recruitment and expansion of neural stem cells (NSCs) from the quiescent pool in the SVZ neurogenic

niche. To this aim, we performed a more thorough analysis of the type B (NSCs) population by analyzing different parameters of type B cells, identified by the concomitant expression of Nestin and Sox2. In 2 month-old mice, we have not found any difference in SVZ volume within different experimental conditions (Supp. Fig. 1A), then the data will be presented as cell density (number of positive cells/SVZ area). Remarkably, in the KO RUN mice, we observed a significant increment of the total number of NSCs (nestin+/sox2+ cells) in comparison with KO NO RUN ($p < 0.001$, Fig. 1a, b) and WT NO RUN mice ($p < 0.001$, Fig. 1b). A similar increment was also detected when we analyzed the proliferating NSCs identified as Ki67+/nestin+/sox2+ cells (KO RUN vs KO NO RUN $p < 0.001$;

KO RUN vs WT NO RUN $p < 0.001$, Fig. 1c). Consistently, in the KO RUN SVZ, we observed an enhancement of the percentage of NSCs recruited from quiescence to the cell cycle (expressed as the ratio between Ki67+/Nestin+/Sox2+ to the total Nestin+/Sox2+) with respect to the KO NO RUN mice ($p < 0.01$ Fig. 1d). As expected, we did not observe any significant pro-neurogenic action exerted by running in the SVZ of wild-type mice; as in 2-month-old WT mice running did not play any beneficial role on the various steps of SVZ neurogenesis; this aspect will not be mentioned hereafter except in graphics. These results clearly indicate that: (a) in a specific condition of defective neurogenesis, such as that caused by the knockdown of the Btg1 gene, an extrinsic neurogenic factor like physical

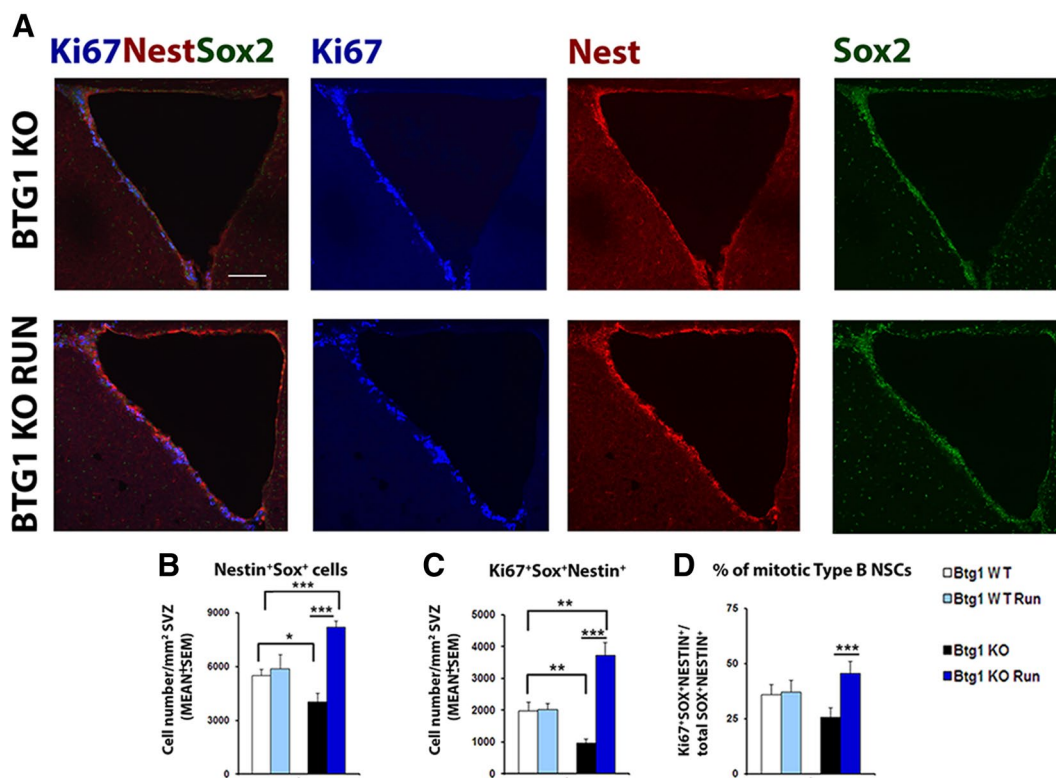


Fig. 1 Expansion of Btg1 knockout NSCs and recruitment from quiescence after 12 days of running. **a** Representative fluorescence images of SVZ coronal sections of Ki67⁺/Nestin⁺/Sox2⁺ triple labeling, in blue, red, and green, respectively, showing the large increase of Type B NSCs in the KO RUN respect to the KO NO RUN mice. Scale bar 100 μ m. **b** Overall number of NSCs identified with the markers Nestin⁺/Sox2⁺ was significantly decreased in KO NO RUN mice if compared with WT NO RUN (genotype \times exercise interaction, $F_{(1,18)} = 22.163$, $p < 0.001$, followed by analysis of simple effect, $*p < 0.05$). Running induces a strong increase of NSCs pool respect with KO NO RUN (genotype \times exercise interaction, $F_{(1,18)} = 22.163$, $p < 0.001$ followed by the analysis of simple effect, $***p < 0.001$) and also WT NO RUN (genotype \times exercise interaction, $F_{(1,18)} = 22.163$, $p < 0.001$ followed by analysis of simple effect, $***p < 0.001$). **c** We observed a very similar pattern also when we analyzed the proliferating fraction of NSCs with a sharp decrease in the KO NO

RUN respect to WT NO RUN (genotype \times exercise interaction, $F_{(1,18)} = 27.075$, $p < 0.001$, followed by analysis of simple effect, $*p < 0.05$) and an enhanced number of proliferating NSCs in KO RUN mice respect to the KO NO RUN (genotype \times exercise interaction, $F_{(1,18)} = 27.075$, $p < 0.001$, followed by the analysis of simple effect, $***p < 0.001$) and to the WT NO RUN mice (genotype \times exercise interaction, $F_{(1,18)} = 27.075$, $p < 0.001$, followed by the analysis of simple effect, $***p < 0.001$). **d** Percentage of type B cells recruited in the cell cycle (ratio between Ki67⁺/Nestin⁺/Sox2⁺ and total Nestin⁺/Sox2⁺ cells) was significantly increased in KO RUN mice in comparison to KO NO RUN mice (genotype \times exercise interaction, $F_{(1,18)} = 5.325$, $p < 0.05$, followed by the analysis of simple effect, $***p < 0.001$). Cell numbers are mean \pm SEM of the analysis of at least three animals per conditions. $*p < 0.05$, $**p < 0.01$, or $***p < 0.001$; ANOVA test

exercise is capable of strongly re-activating SVZ neurogenesis; (b) this event, never observed before in the SVZ, is probably dependent on the increased recruitment of quiescent NSCs as well as on their proliferative activation; (c) the lack of the antiproliferative inhibition exerted by Btg1 might allow the NSCs to retain or express a considerable neurogenic potential able not only to restore the impaired proliferation of Nestin⁺/Sox⁺ NSCs but also to expand the stem cell pool in the SVZ after a pro-neurogenic stimulus, such as running.

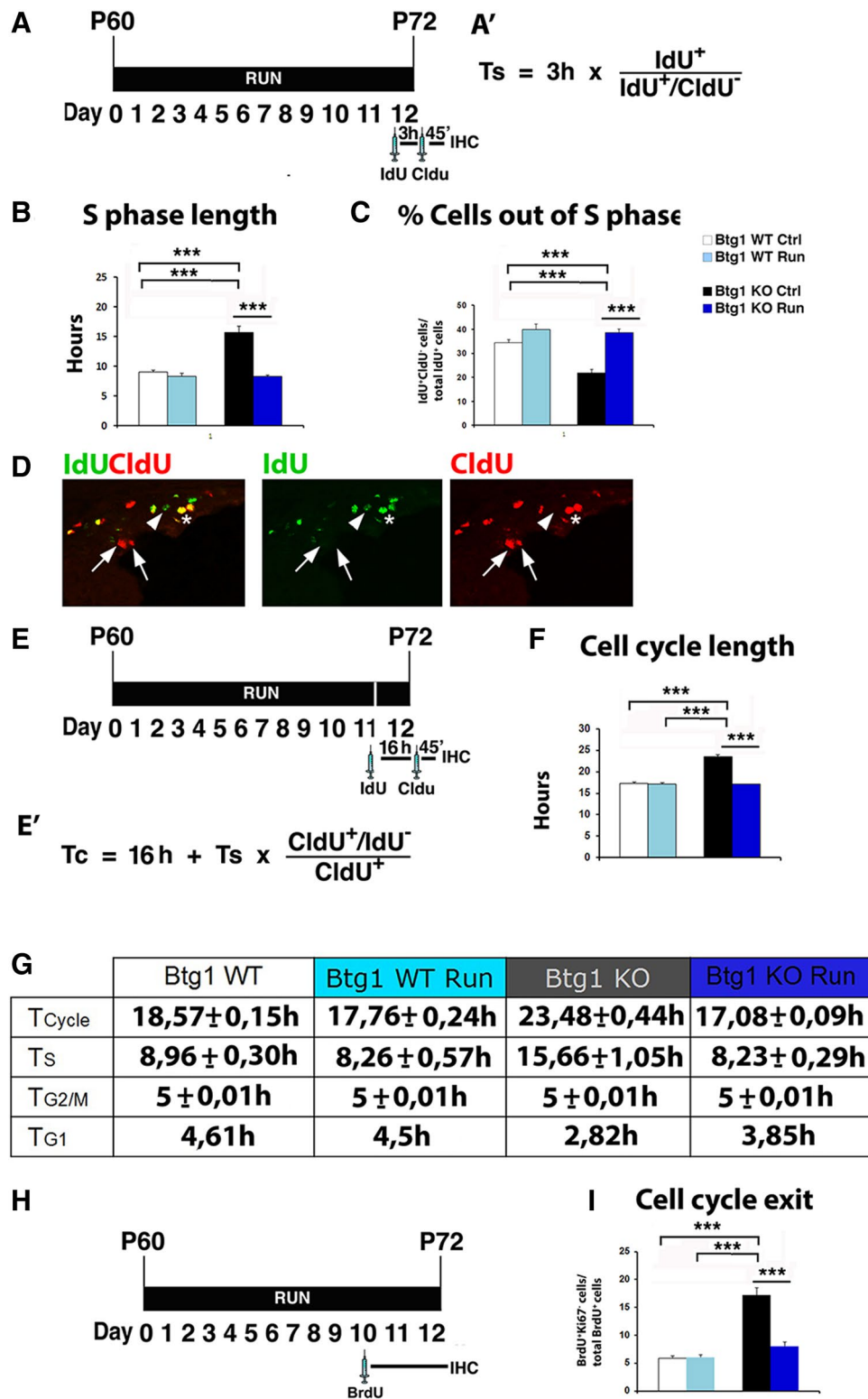
Effects of physical activity on cell cycle parameters in the Btg1 null mice

To ascertain if the running-dependent increment of cell division in the SVZ of Btg1 KO mice was correlated with modifications of cell cycle kinetics in the different stages of SVZ newly generated neurons, we decided to perform a precise calculation of cell cycle length of proliferating cells, by adopting, with few modifications, a method previously developed by Brandt et al. for measuring the cell cycle length in the dentate gyrus (Brandt et al. 2012). This method utilizes two different intervals between injections of two BrdU analogs, IdU and CldU, to precisely calculate the S-phase length (3-h interval, T_s , Fig. 2a, a') and total cell cycle length (16-h interval, T_c , Fig. 2e, e'). By this analysis, we measured in the WT NO RUN mice $T_s = 8.9 \pm 0.3$ h (Fig. 2b, g) and determined that $34.5\% \pm 1.15$ cells had exited from the S-phase during the 3-h interval (Fig. 2c), while the average length of whole cell cycle was $T_c = 18.5 \pm 0.15$ h (Fig. 2f, g). In the KO NO RUN, we detected a significant lengthening of the S-phase duration respect to the WT NO RUN ($T_s = 15.6 \pm 1.43$ h $p < 0.001$, Fig. 2b, g) with a large decrease of cells out from the S-phase ($21.8\% \pm 1.05$ h, $p < 0.001$, Fig. 2c) and a concomitant increment of cell cycle duration ($T_c = 23.4 \pm 0.44$ h, $p < 0.001$, Fig. 2f, g). The voluntary running induced, in the Btg1 KO mice, a significant reduction of the S-phase length ($T_s = 8.0 \pm 0.26$ h, Fig. 2b, g) compared to KO NO RUN and also to WT NO RUN mice (in both cases $p < 0.001$), while the percentage of cells that had left the S-phase ($39.5\% \pm 1.44$) was almost double with respect to the KO NO RUN ($p < 0.001$, Fig. 2c) and significantly higher than that observed in the WT NO RUN mice ($p < 0.001$, Fig. 2c). The running-induced high rate of S-phase acceleration, in turn, resulted in a significantly shorter cell cycle length in the KO RUN (17.1 ± 0.09 h), in comparison with the Btg1 KO sedentary mice ($p < 0.001$, Fig. 2f, g), re-establishing the physiological cell cycle length observed in the WT NO RUN mice. We did not detect any difference when we compared the cell cycle kinetics between WT NO RUN and WT RUN. These data showed that in the SVZ of KO RUN mice, the concomitant effects of physical exercise and

the lack of the inhibition of proliferation exerted by Btg1 resulted in a considerable shortening of the S-phase. This event triggers a faster progression of cycling cells and promotes a shorter duration of the overall cell cycle, thereby inducing an increase of the proliferation rate. However, it cannot be excluded that other phases of the cell cycle may contribute substantially to the shortening of the length of the cell cycle. To investigate this possibility, we calculated the length of the G2/M phase, by adopting the percentage of labeled mitotic cells (for further information, see M&M) and we found that the length of G2 + M phases was about 5 h for all the experimental groups taken in consideration (Fig. 2g). Moreover, the calculation of the G1 phase obtained by subtraction from the T_c of the S-phase and G2/M phases did not reveal significant differences between the various experimental conditions (Fig. 2g). Finally, as expected, we did not find any significant changes of cell cycle kinetics in WT RUN mice when compared with the sedentary counterparts.

To obtain a more exhaustive picture of the role played by exercise in determining the increase in the proliferation of the different subpopulation of the SVZ in the Btg1 KO mice, we evaluated the cell cycle length in the type B NSCs as well as in the Type A neuroblasts, by combining triple immunolabeling (IDU/CldU/GFAP for type B cells and IdU/CldU/Dcx for type A cells) using the method described above. Our data demonstrated that Btg1 KO mice showed a significant lengthening of S-phase both in the GFAP⁺ and in the Dcx⁺ sub-populations when compared with their WT littermates ($p < 0.001$ for GFAP Fig. 3a, b, d and Dcx, Fig. 3g, h, j), which resulted in a significant lengthening of the cell cycle duration ($p < 0.001$ for GFAP, Fig. 3a, b, d and Dcx, Fig. 3g, h, j). The exercise strongly affected the cell cycle kinetics in the Btg1 KO RUN mice, by reverting to WT NO RUN levels the S-phase and the whole cell cycle duration in the type B (GFAP⁺) and type A (Dcx⁺) cells. Consequently, a specific action of voluntary running in the KO RUN mice was represented by a significantly shorter T_s in the GFAP⁺ and DCX⁺ cells, in comparison to KO NO RUN mice ($p < 0.001$ for GFAP, Fig. 3a, b, d, e and Dcx, Fig. 3g, h, j, k), which results in a significantly shorter T_c in both the sub-populations ($p < 0.001$ for GFAP, Fig. 3a, b, d, e and Dcx, Fig. 3g, h, j, k). In addition, in this case, we did not observe significant changes in the duration of G2/M and G1 phases between the different conditions. Overall, these data highlighted the role of cell cycle kinetics, and in particular of the S-phase duration, as a key component to mediate the pro-neurogenic effect of running in the replenishment of the pool as well as in the increased proliferation observed in the SVZ of Btg1 KO RUN mice.

We wished also to ascertain whether a shorter period of physical exercise (5 days of running), representing a more acute stimulus, was able to exert a pro-neurogenic effect



on the SVZ of Btg1 KO mice similar to that observed with the paradigm of 12 days of running. To do this, we analyzed the proliferation rate (Ki67⁺ cells), the size of the neural stem cells pool (by immunolabeling with Ki67/Nestin), and the progenitor cells number (by immunolabeling

with Ki67/DCX) in the SVZ of Btg1 KO mice after 5 days of running. We found a significant increase of cell proliferation respect to the KO NO RUN mice (Ki67⁺ cells, $p < 0.01$, Suppl. Figure 2A) with a concomitant expansion of type B (GFAP⁺, Ki67⁺/GFAP⁺ cells, $p < 0.01$ for both

Fig. 2 Cell cycle length analysis reveals a running-dependent shortening of S-phase in the Btg1 knockout mice. **a** Experimental timeline of thymidine analog pulses for S-phase measurement. Mice were put in the running cage for 12 days. On the last day, mice received double pulses of IdU and CldU and perfused after 45 min from the second injection, as explained in detail in “Material and methods”. **a'** Equation for the length of S-phase. The ratio of cells that have left S-phase during the 3 h of interinjection interval ($\text{IdU}^+/\text{CldU}^-$ cells) to the total number of IdU^+ cells is equal to 3 h/Ts. **b** Histogram showing S-phase duration among the four different experimental conditions. While in KO NO RUN mice, we measured a very strong increment of the duration of S-phase (Ts) when compared to WT NO RUN (genotype \times exercise interaction, $F_{(1,117)}=29.677$, $p < 0.001$, followed by the analysis of simple effect, $***p < 0.001$), 12 days of running is able to recover the S-phase length (KO RUN vs KO NO RUN, genotype \times exercise interaction, $F_{(1,117)}=29.677$, $p < 0.001$, followed by the analysis of simple effect, $***p < 0.001$) to physiological levels detected in WT NO RUN. **c** Graph representing the fraction of cells out of S-phase calculated with the double pulse method (ratio of the $\text{IdU}^+/\text{CldU}^-$ to the IdU^+ total cells). In BTG1 KO NO RUN, a significant increase of cells remained in S-phase occurred when compared with the WT NO RUN mice (genotype \times exercise interaction, $F_{(1,117)}=15.291$, $p < 0.001$, followed by the analysis of simple effect, $***p < 0.001$); running induces an increase of cell cycle exit in the BTG1 KO mice compared with their sedentary littermates (genotype \times exercise interaction, $F_{(1,117)}=15.291$, $***p < 0.001$, followed by the analysis of simple effect, $***p < 0.001$), re-establishing the correct timing of cell cycle kinetics. **d** Interval of 16 h between IdU and CldU injections produces cycling cells that were in S-phase during the IdU injection only ($\text{IdU}^+/\text{CldU}^-$ cells, green, arrowhead), or during the CldU pulse ($\text{IdU}^-/\text{CldU}^+$ cells, red, arrow), or cells that re-entered in the cell cycle and were in S-phase during both the pulse ($\text{IdU}^+/\text{CldU}^+$, yellow, asterisk). **e** Experimental timeline of thymidine analog pulse for the precise measurement of the whole cell cycle length from Brandt et al. (2012) with our modification. For more detailed information, see Material and Methods. **e'** Equation for the calculation of the cell cycle with the IdU/CldU method. **f** Histogram showing the cell cycle measurement in the different experimental conditions. Running is able to restore to the physiological level the cell cycle lengthening observed in the BTG1 KO respect to the WT NO RUN (WT CTL vs KO NO RUN, genotype \times exercise interaction, $F_{(1,50)}=105.250$, $***p < 0.001$, followed by the analysis of simple effect, $***p < 0.001$; KO RUN vs KO NO RUN, genotype \times exercise interaction, $F_{(1,50)}=105.250$, $p < 0.001$, followed by the analysis of simple effect, $***p < 0.001$). **g** Table illustrating the length of total cell cycle, S-phase, G2/M phase, and G1 phase among the different experimental conditions. All data are showed as means \pm SEM except TG1 value. **h** Experimental timeline of BrdU pulse for cell cycle exit calculation. Mice were injected with BrdU on the tenth day of running and sacrificed 48 h later. **i** Histogram shows the precocious exit from the cell cycle of type A cells of Btg1 KO NO RUN mice, which is totally reverted by running (WT NO RUN vs KO NO RUN, genotype \times exercise interaction, $F_{(1,41)}=16.881$, $***p < 0.001$, followed by the analysis of simple effect, $***p < 0.001$; KO RUN vs KO NO RUN, genotype \times exercise interaction, $F_{(1,41)}=16.881$, $p < 0.001$, followed by the analysis of simple effect, $***p < 0.001$). Cell numbers are mean \pm SEM of the analysis of at least three animals per conditions. $***p < 0.001$; ANOVA test

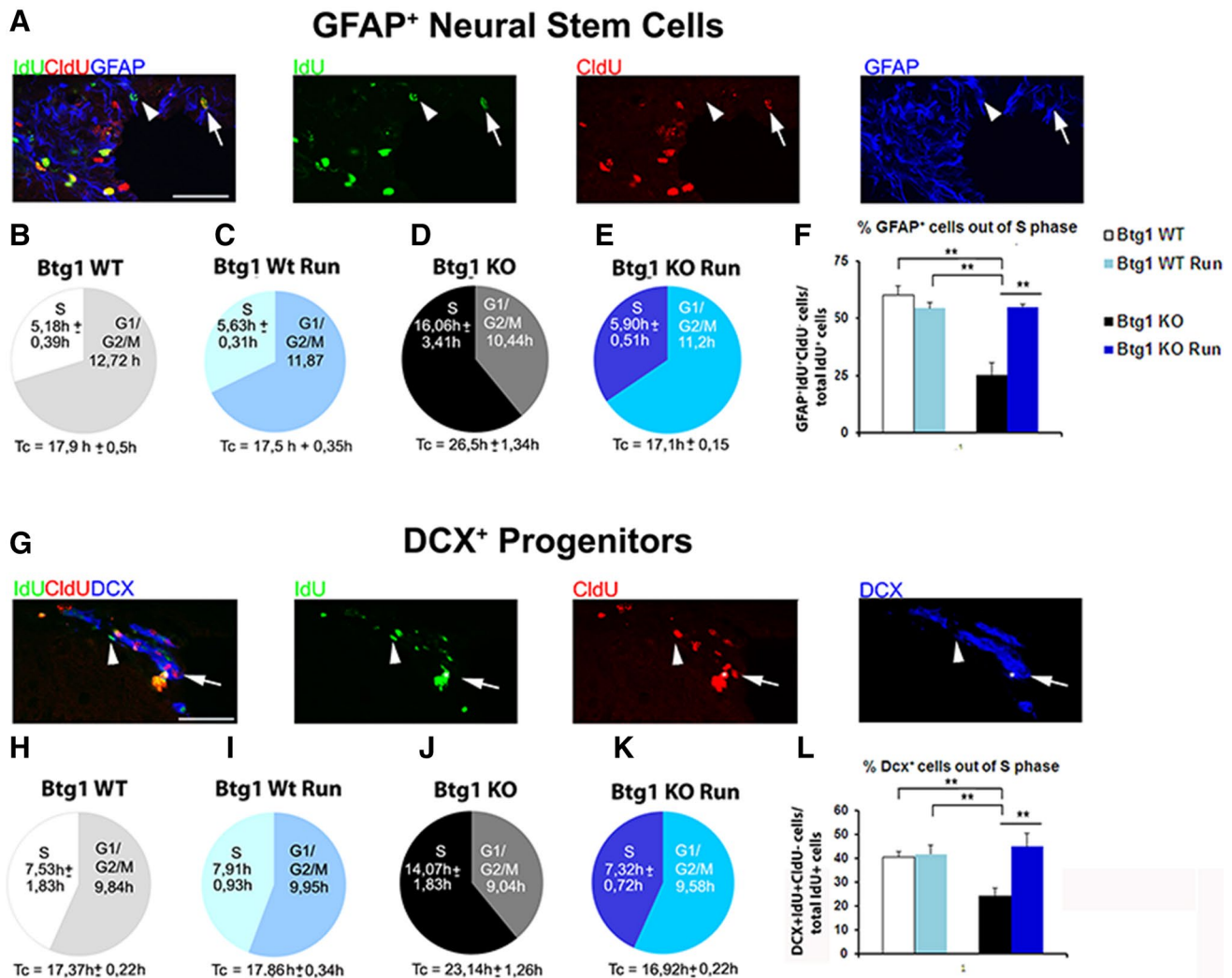
the markers, Suppl. Figure 2B, D) and type A pool (DCX^+ , $\text{Ki67}^+/\text{DCX}^+$ cells, $p < 0.01$ and $p < 0.05$, respectively, Suppl. Figure 2C, E), resulting in a complete restoration of SVZ neurogenesis to the values of Btg1 WT mice. However, our data strongly stated that 5 days of running were

not sufficient to trigger the over-proliferation and the stem cell and progenitor cell increase induced after 12 days of running in the SVZ of Btg1 KO mice, which displayed a significantly increased subventricular neurogenesis in comparison with the values measured after 5 days of physical activity (Suppl. Figure 2).

The previous data have correlated the declined proliferation in the dentate gyrus of Btg1 KO mice with a premature exit of neural progenitor from the cell cycle. Thus, we predicted that reduction in proliferation of SVZ stem/progenitors in the Btg1 KO mice was also due to a defect in the cell cycle exit. To investigate this, we determined the cell cycle exit for neuroblasts in the SVZ. Animals were injected with BrdU and sections immunostained for BrdU and Ki67 48 h later (Fig. 2h). The proportion of cells exiting the cell cycle over this period was calculated by dividing the number of BrdU+/Ki67 cells by the total number of BrdU+ cells. The data obtained showed that in the Btg1 KO mice, the percentage of newborn neurons out of cell cycle after 48 h increased largely in comparison with the Btg1 WT mice (about threefold, from 6 to 17%; $p < 0.001$ Fig. 2i), while running partially restored the cell cycle exit value to the level observed in the WT mice (8%) (Btg1 KO RUN vs Btg1 KO $p < 0.001$ Fig. 2i). We also analyzed the effect of 5 days of running on the cell cycle kinetic in the Btg1 KO mice, and we observed that even after 5 days of running, there is a significant reduction of S-phase and an increase of the percentage exited from the S-phase in the RUN Btg1 KO mice against the sedentary control ($p < 0.001$ for both the parameters, Suppl. Figure 3A, B), which results in a concomitant shortening of the whole cell cycle with respect to the Btg1 KO mice ($p < 0.05$, Suppl. Figure 3C). The cell cycle analysis suggested that in the SVZ of Btg1 KO mice, the combined effect of cell cycle lengthening and anticipated exit from the cell cycle induced a reduction of the replicative cycles and consequently a significant impairment of proliferation of the stem/progenitor cells. In the BTG1 KO mice, running is able to totally revert this phenotype, by shortening cell cycle length, and by allowing the cells to remain longer in the cycle and make a greater number of cell divisions. These events involved a dramatic increase in the number of neural stem cells in the SVZ Btg1 mice that is reflected in a general enhancement of subventricular neurogenesis.

The early migration from SVZ of Btg1 KO neuroblasts is totally reverted by running

Adult-generated neurons, once they are originated in the SVZ, migrate through a complex path of migration, named rostral migratory stream (RMS), to their final destination the olfactory bulb (OB), where they fully mature mostly into GABAergic local interneurons called granule cells



(GCs). We asked whether the different cell cycle kinetics observed in the experimental conditions could play an instructive role in the migratory dynamics of the post-mitotic progenitors. To this end, sedentary and running mice were treated with 5 daily injections of BrdU, followed by sacrifice 7 days after the last injection (Fig. 4a). During the period of 12 days, the BrdU⁺ newborn neurons are distributed along the caudal-rostral path SVZ-RMS-OB with a well-coordinated migration pattern and with the expression of specific cell markers, such as PSA-NCAM and DCX (Fig. 4b). To determine the migration kinetic of the post-mitotic neuroblast in the different experimental conditions, we counted BrdU⁺/DCX⁺ cells in the different regions of neuroblast migration from caudal to rostral comprising SVZ, RMS, infrabulbar OB, and OB, and we calculated their relative fraction of the sum of BrdU⁺ cells counted in all the areas analyzed. We utilize this count method because of the wide variability of BrdU⁺ cells originating from the SVZ in the different experimental conditions. By this analysis, we observed that in the Btg1 KO

mice, the migrating neuroblasts have a greater distribution in the rostral regions, infrabulbar RMS, and OB, and are almost absent in the SVZ, in comparison with the distribution detected in the WT mice which displays a much more homogeneous distribution of BrdU⁺ cells among the different regions analyzed (RMS (OB) $p < 0.05$; OB $p < 0.05$; SVZ $p < 0.001$; Fig. 4c, d), suggesting that in Btg1 KO mice, an anticipated migration occurred, probably due to an early exit from the cell cycle. The altered pattern of migration examined in the Btg1 KO mice is totally reverted by running, which is able to re-establish a distribution of migrating neuroblasts comparable to that observed in the WT mice, confirming a specific and causal tempo-spatial coordination between cell cycle exit and migration (KO NO RUN vs KO RUN: RMS (OB) $p < 0.01$; OB $p < 0.01$; SVZ $p < 0.001$; Fig. 4c, d).

These data, however, did not fully clarify if the anticipated migration observed in the BTG1 KO mice and the pattern restoration after running is a cell-autonomous effect or it is dependent on the extracellular environment, which

Fig. 3 Effect of running on cell cycle length of GFAP⁺ and DCX⁺ cell populations. **(a)** Representative confocal image of triple labeling with IdU (green), CldU (red), separated by 3 h, and GFAP (blue). A GFAP⁺ cell (blue) is shown that was in S-phase during both injections (IdU⁺ green and CldU⁺ red, arrowhead). The arrow indicates a GFAP⁺ NSCs (blue) that exited S-phase between the two injections (IdU⁺ green and CldU⁻). Scale bar 525 mm. **b–e** Panels representing the measured S-phase, G2/M phase and cell cycle length for the stem GFAP⁺ cell population in the different experimental conditions, showing a lengthening of Ts and Tc in the KO NO RUN mice with respect to WT NO RUN mice (Ts WT NO RUN vs KO NO RUN, genotype × exercise interaction, $F_{(1,28)} = 11.403$, $p < 0.01$, followed by the analysis of simple effect, $***p < 0.001$; Tc WT NO RUN vs KO NO RUN, genotype × exercise interaction, $F_{(1,28)} = 39.194$, $p < 0.001$, followed by the analysis of simple effect, $***p < 0.001$). Running is able to totally revert the Ts and Tc duration, re-establishing the normal value observed in the WT NO RUN mice (Ts, KO RUN vs KO NO RUN, genotype × exercise interaction, $F_{(1,28)} = 15.649$, $p < 0.001$, followed by the analysis of simple effect, $***p < 0.001$; Tc, KO RUN vs KO NO RUN, genotype × exercise interaction, $F_{(1,28)} = 39.194$, $p < 0.001$, followed by the analysis of simple effect, $***p < 0.001$). **f** Histogram showing the percentage of GFAP⁺ cells out of S-phase (WT NO RUN vs KO NO RUN, genotype × exercise interaction, $F_{(1,28)} = 15.649$, $p < 0.001$, followed by the analysis of simple effect, $***p < 0.001$, KO RUN vs KO NO RUN, genotype × exercise interaction, $F_{(1,28)} = 15.649$, $p < 0.001$, followed by the analysis of simple effect, $***p < 0.001$). **g** Representative confocal image of triple labeling with IdU (green), CldU (red), separated by 3 h, and DCX (blue). In this example, the asterisk indicates a DCX⁺ cell (blue) that was in S-phase during both injections (IdU⁺ green and CldU⁺ red), the arrowhead displays a DCX⁺ neuroblast (blue) that exited S-phase between the two injections (IdU⁺ green and CldU⁻), and the arrow shows a DCX⁺ cells that entered S-phase during the 3-h injections interval (IdU⁻ and CldU⁺ red). Scale bar 525 mm. **h–k** Panels representing the measured S-phase, G2/M phase, and cell cycle length for the neuroblasts DCX⁺ cell population in the different experimental conditions. The graphs show a lengthening of Ts and Tc in the KO NO RUN mice with respect to WT NO RUN mice (Ts, genotype × exercise interaction, $F_{(1,28)} = 9.381$, $p < 0.01$, followed by the analysis of simple effect, $***p < 0.001$; Tc, genotype × exercise interaction, $F_{(1,28)} = 20.753$, $p < 0.001$, followed by the analysis of simple effect, $***p < 0.001$). In addition, in this case, running reverts the Ts and Tc duration, re-establishing the physiological cell cycle parameter observed in the WT NO RUN mice (Ts, genotype × exercise interaction, $F_{(1,32)} = 9.381$, $p < 0.01$, followed by the analysis of simple effect, $***p < 0.001$; Tc, KO RUN vs KO NO RUN, genotype × exercise interaction, $F_{(1,28)} = 20.753$, $p < 0.001$, followed by analysis of simple effect, $***p < 0.001$). **l** Histogram showing the percentage of DCX⁺ cells out of S-phase (WT NO RUN vs KO NO RUN, genotype × exercise interaction, $F_{(1,28)} = 5.714$, $p < 0.05$, followed by the analysis of simple effect, $*p < 0.05$; KO RUN vs KO NO RUN, genotype × exercise interaction, $F_{(1,28)} = 5.714$, $p < 0.05$, followed by analysis of simple effect, $***p < 0.001$). Cell numbers are mean ± SEM of the analysis of at least three animals per conditions. $*p < 0.05$, $**p < 0.01$ or $***p < 0.001$. ANOVA analysis. SVZ subventricular zone, RMS rostral migratory stream, OB olfactory bulb, GFAP glial fibrillary acidic protein, DCX doublecortin, IdU 5-iodo-2-deoxyuridine, CldU 5-chlorodeoxyuridine

played a pivotal role in regulating the neuroblast migration. To assess this point, we compared the migration capacity in the different conditions using Matrigel assays, which show neuroblast migration in chains in vitro (Witcherle et al. 1997). Our data demonstrated a striking increase of

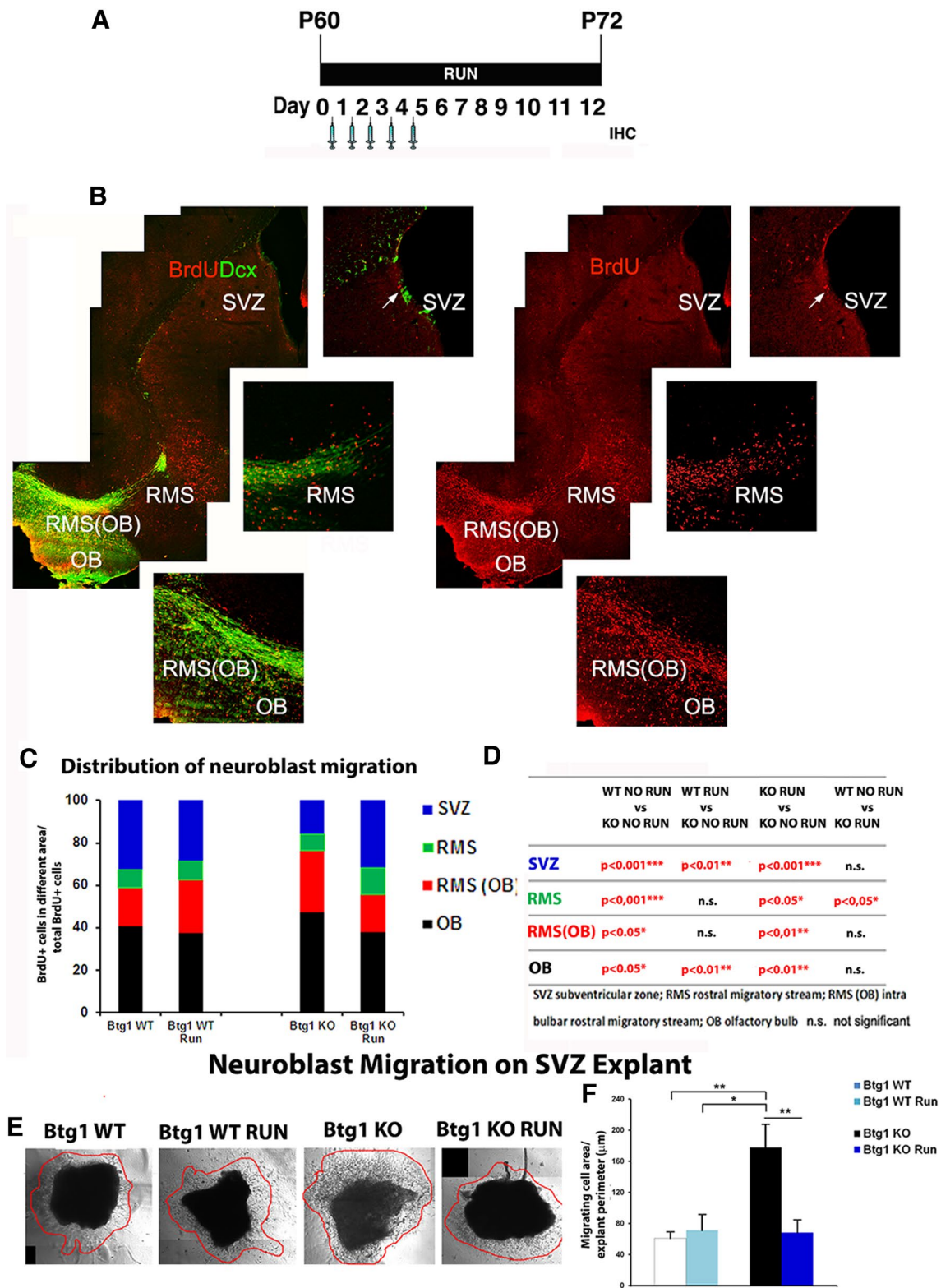
migration after 8 days in vitro from the explant in the Btg1 KO mice with respect to the WT mice ($p < 0.01$ Fig. 4e, f), while running totally restores the migration pattern away from the explants at the comparable level observed in the WT mice (KO RUN vs KO NO RUN $p < 0.01$; KO RUN vs WT NO RUN n.s., Fig. 4e, f), confirming the in vivo data and suggesting that in Btg1 KO mice, running might act to synchronize cell cycle exit and neuroblast migration.

Running restores the impaired terminal differentiation and the enhanced apoptotic cell death in the OB of Btg1 KO mice

Migration analysis revealed that the lack of Btg1 expression induced the neuroblasts to prematurely enter in the OB. Therefore, we asked whether the deregulated migration pattern in Btg1 KO mice may have some negative influence on neuroblast terminal differentiation and survival. With this aim, we analyzed the number of 12-day-old BrdU + NeuN + neurons in the granules cell layer (GCL) of OB, and we found that in Btg1 KO mice, the fraction of terminally differentiated newly generated neurons (expressed as the ratio between BrdU⁺NeuN⁺/total BrdU⁺ in the GCL of OB, Fig. 5a) was strikingly decreased in comparison with the WT mice ($p < 0.01$ Fig. 5d). Moreover, the analysis with the apoptotic marker Caspase-3 revealed a large increase of apoptotic cell death in the cell population residing in the GCL of Btg1 KO mice when compared with the WT NO RUN mice ($p < 0.001$ Fig. 5b, c, e). Physical activity provided a beneficial effect on terminal maturation of Btg1-devoid newly generated neurons; indeed, we observed, in BTG1 KO RUN mice, an increase of percentage of BrdU⁺NeuN⁺ cells and a concomitant decrement of caspase-3⁺ cells when compared to the Btg1 KO mice ($p < 0.001$ both for BrdU⁺NeuN⁺ and caspase-3 Fig. 5b, c, e), reaching the physiological levels detected in the WT mice.

Role of running in the survival and functional activation of newly generated neurons of Btg1 null mice

In the OB, 3–4 weeks after their arrival, newborn GCs fully mature into GABAergic inhibitory neurons, which modulate mitral/tufted cells. It is widely recognized that adult-born OB neurons are specifically recruited and activated by odor stimulation. This evidence was clearly supported by the mapping of the immediate early gene (IEG) c-fos, a marker of cellular activation that has previously been used to image activation within the OB. In our study, we wished to determine if the anticipated migration of neuroblasts and the consequent impairment in differentiation observed in the OB of Btg1 KO mice had a negative effect on the recruitment of OB newborn neurons after



olfactory stimulation. To this end, mice were treated with 5 daily injections of BrdU and then underwent olfactory stimulation 4 weeks later. Mice were sacrificed 1.5 h after the stimulation, and the number of new neurons activated

was measured by concomitant positivity to BrdU NeuN and c-fos (Fig. 5f, g). In BTG1 KO mice, the number of 4-week-old neurons of (BrdU⁺/NeuN⁺) was significantly reduced in comparison with that observed in the Btg1 WT

Fig. 4 Effect of physical activity on neuroblast migration. **a** Experimental timeline of BrdU pulses for migration analysis. Mice were injected with single doses of BrdU the first 5 days of running and sacrificed 7 days after the fifth injection. **b** Representative image showing the migration path of the post-mitotic neuroblasts from the subventricular zone to the olfactory bulb. Migrating neuroblasts have been identified with the double labeling BrdU / DCX, while new neurons arrived in the bulb are BrdU⁺ DCX⁻. To assess differences in the migration kinetic of neuroblasts in the four experimental groups, we calculated the fraction of BrdU⁺ cells in the four main districts of the migration path (SVZ, RMS, intrabulbar RMS, and OB) respect the total BrdU⁺ cells present in the whole migration path. **c** Quantification of BrdU⁺ cells distribution in the different areas of migratory route [SVZ, RMS, RMS (OB), and OB], clearly showing that physical exercise totally recovers to physiological levels the anticipated migration pattern of post-mitotic neuroblasts in the Btg1 KO mice. **d** ANOVA analysis reports genotype × exercise effects (G × T), followed by the analysis of the simple effects. **e** Representative live-imaging images of the four experimental conditions. After 8 days of culture in Matrigel, we observed a striking increase of neuroblast migration in the KO NO RUN explants. Running totally restores the migration pattern. Scale bar 150 μm. The red lines indicate the border of the migrating area (**b**). Histogram showing the quantification of migrating cells per area in all experimental conditions (WT NO RUN vs KO NO RUN, genotype × exercise interaction, $F_{(1,32)}=4.029$, $p<0.05$, followed by the analysis of simple effect, $**p<0.01$; KO RUN vs KO NO RUN, genotype × exercise interaction, $F_{(1,32)}=4.029$, $p<0.05$, followed by the analysis of simple effect, $**p<0.01$). Cell numbers are mean ± SEM of the analysis of at least three animals per conditions. $*p<0.05$, $**p<0.01$ or $***p<0.001$. *ns* not significant, *SVZ* subventricular zone, *RMS* rostral migratory stream, *OB* olfactory bulb

mice ($p<0.001$, Fig. 5h). We observed a similar decrease when we counted the numbers of activated 4-week-old newly generated neurons (BrdU⁺/NeuN⁺/c-fos⁺), if compared with the recruited new neurons expressed in the OB of Btg1 WT mice ($p<0.05$, Fig. 5j). In the KO RUN mice, we found not only a complete restoration of the number of 4-week new neurons (BrdU⁺/NeuN⁺) to a value comparable with the WT mice, but we detected a significant increase in the number of c-fos⁺ new neurons in the OB in comparison not only with Btg1 KO ($p<0.001$, Fig. 5j) but also with the BTG1 WT mice ($p<0.05$, Fig. 5j). In addition, the total number of c-fos activated neurons was increased Btg1 KO mice after running ($p<0.001$, Fig. 5i). Overall, the pattern of c-fos immunoreactivity in the OB new neurons strongly suggests that the positive effect exerted by physical activity to the NSCs pool in the SVZ of Btg1 KO not only normalizes the physiological neurogenic progression of new cells, but also increases over the physiological level the fraction of new neurons ready to be activated after an exogenous stimulus, such as olfactory stimulation.

In vitro analysis of the effect of running in the Btg1-devoid SVZ

We have previously shown that the lack of Btg1 affected in vitro both the self-renewal and the proliferative capacity

of neural stem progenitors (NSPs) isolated from SVZ of adult Btg1 KO mice. This effect was due in part to the impairment of asymmetric division in NSPs derived from BTG1 KO SVZ, which resulted in decrease of NSPs pool size and proliferative capacity (Farioli-Vecchioli et al. 2012). In this study, we examined the in vitro effect of physical exercise on the neurospheres isolated from the SVZ of adult (2 months old) Btg1 wild-type and knockout mice. As a first step, we determined the relationship between exercise and adult neural progenitors behavior in vitro using the neurosphere assay in the different conditions under investigation. In exercised WT mice, we did not observe any increase in SVZ-derived primary neurosphere number compared to WT mice without access to the running wheel, while we detected a significant increment of neurosphere-forming cell population derived from SVZ of KO RUN mice when compared with the other experimental conditions (KO RUN vs KO $p<0.001$; KO RUN vs WT $p<0.05$, Fig. 6a, b). These findings are fully in agreement with in vivo data, suggesting that exercise in the Btg1 KO mice is able not only to fully recover the stem cell exhaustion in the SVZ but also to trigger an unexpected activation and expansion of the NPCs pool over the values observed in WT and WT RUN mice. To further analyze the previous observations, we wished to investigate the rate of symmetric and asymmetric division of NPCs in the sedentary and exercised mice of both genotypes, by performing secondary neurosphere assays. Indeed, under physiological conditions, asymmetric cell division allows the NPCs pool to maintain approximately the same size, while the result of symmetric division is the generation of the NPCs daughter cells, thereby expanding the NPCs pool. After mechanical dissociation of primary neurospheres, we seeded them at low density and calculated the size of secondary neurospheres, as indication of symmetric division, after 7 days of culture. The data obtained clearly showed that the secondary neurospheres from KO RUN were significantly larger compared to the KO mice ($p<0.001$, Fig. 6a, c) and to the sedentary WT mice ($p<0.001$, Fig. 6a, c), reflecting the large increase of self-renewing as causal effect of physical exercise in the secondary neurospheres from Btg1 KO RUN mice.

However, the capacity of expansion and proliferation shown by NSCs isolated from SVZ of KO RUN mice led to a rapid and dramatic exhaustion of the pool with passaging of secondary neurospheres, as indicated by the growth curve analysis. In fact, during the five passages of growth curve, the KO RUN mice secondary neurospheres rapidly lost the ability to form new neurospheres as indicated by the drop of the growth curve slope in the KO RUN mice, reaching values significantly lower compared to the KO mice (Fig. 6e). Moreover, from the study of the neurospheres volume at the end of passage 5, we detected a

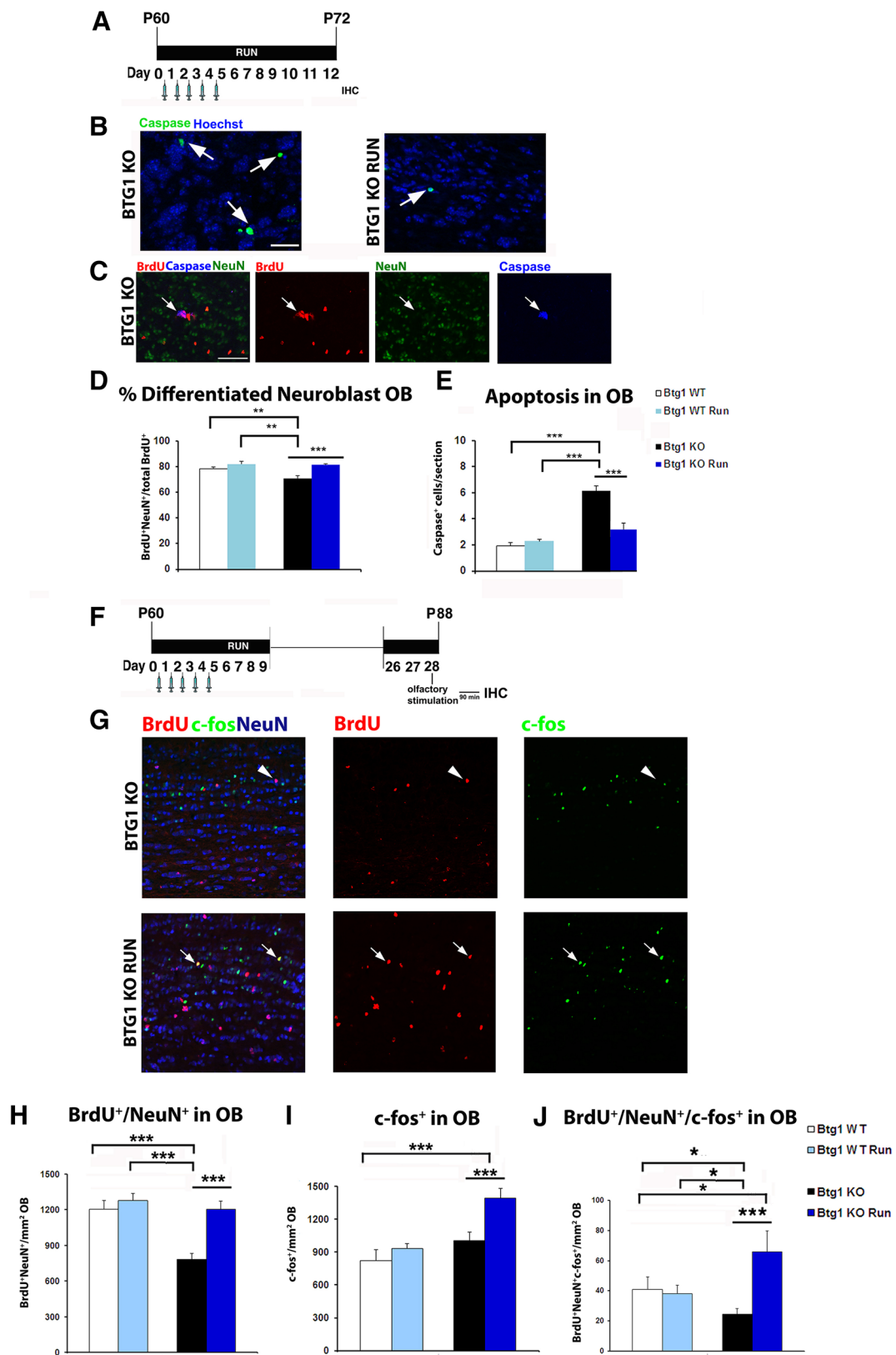
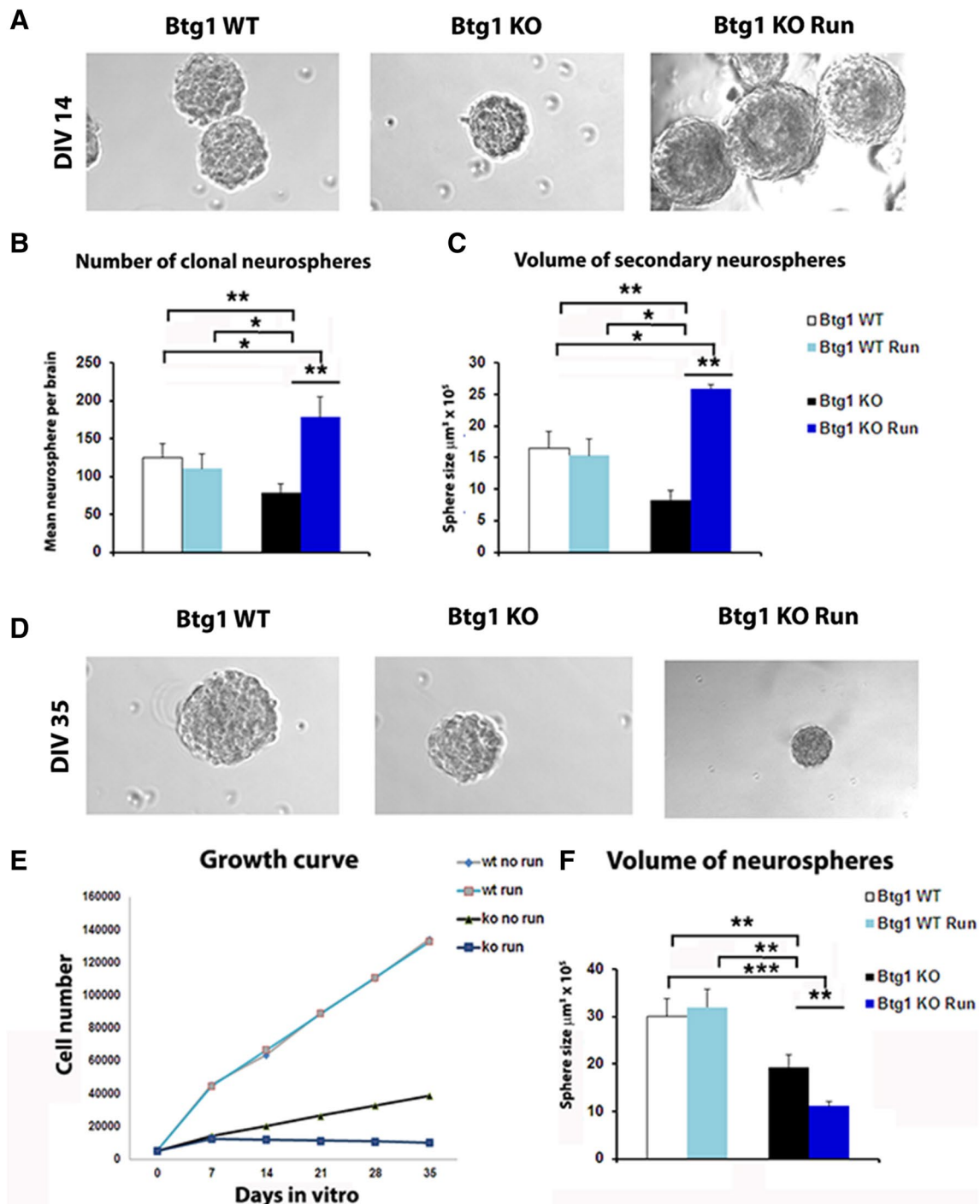


Fig. 5 Effect of running on neuroblast differentiation, survival and functional integration. **a** Experimental timeline of BrdU pulses used to study terminal differentiation and apoptotic death of newborn neurons in OB. Mice were injected with BrdU (95 mg/Kg i.p.) for 5 days and sacrificed the twelfth day. **b** Representative confocal images showing the striking decrease of apoptotic Caspase-3⁺ cells (arrow, green cells) in the granule cell layer of a Btg1 KO RUN olfactory bulb in comparison with the Btg1 KO NO RUN. **c** Triple immunofluorescence confocal images representing an apoptotic (caspase-3⁺, blue) newly generated neurons (BrdU⁺, red), with a defective differentiation (NeuN⁻) in the olfactory bulb of Btg1 KO NO RUN mice. Scale bar 50 μm. **d** Histogram showing the percentage of differentiated neuroblasts in OB, expressed as ratio between BrdU⁺/NeuN⁺ cells and BrdU⁺ cells in the OB. While the absence of Btg1 reduces the percentage of differentiated neuroblasts with respect to the WT NO RUN mice, physical exercise allows re-establishment of the physiological value of newborn neurons differentiation (WT NO RUN vs KO NO RUN, genotype × exercise interaction, $F_{(1,48)}=4.582$, $p<0.05$, followed by the analysis of simple effect, $***p<0.001$; KO RUN vs KO NO RUN, genotype × exercise interaction, $F_{(1,48)}=4.582$, $p<0.05$, followed by analysis of simple effect, $***p<0.001$). **e** Histogram showing that running is able to reduce to the physiological levels the high rise of apoptotic cell death (caspase-3⁺ cells) observed in KO NO RUN with respect to the WT NO RUN mice (WT NO RUN vs KO NO RUN, genotype × exercise interaction, $F_{(1,38)}=6.261$, $p<0.05$, followed by analysis of simple effect, $***p<0.001$, KO RUN vs KO NO RUN, genotype × exercise interaction, $F_{(1,38)}=6.261$, $p<0.05$, followed by the analysis of simple effect, $***p<0.001$). **f** Experimental timeline of BrdU pulses used to study the functional recruitment of newborn neurons. For more detailed information, see “Material and methods” section (**g**). Representative confocal images of coronal sections of olfactory bulb showing in Btg1 KO mice after 12-days of running the presence of functionally integrated newborn SVZ neurons identified with the triple labeling BrdU⁺ red, c-fos⁺ green, and NeuN⁺ blue (arrows). Note in the upper 3 panels representing the OB of KO NO RUN mice, the absence of newborn neurons functionally activated (BrdU⁺ red, NeuN⁺ blue, c-fos⁻, arrowheads) after the odor stimulation. Scale bar 50 μm. **h** Histogram showing the significant increase of BrdU⁺/NeuN⁺ cells in the olfactory bulb after physical exercise in the Btg1 KO RUN with respect to their sedentary littermates (KO RUN vs KO NO RUN, genotype × exercise interaction, $F_{(1,58)}=5.478$, $p<0.05$, followed by the analysis of simple effect, $***p<0.001$), that reverts the striking depletion on newborn OB neurons observed in the KO NO RUN mice with respect to the WT NO RUN mice (genotype × exercise interaction, $F_{(1,58)}=5.478$, $p<0.05$, followed by the analysis of simple effect, $***p<0.001$). **i** Number of OB neurons activated (c-fos⁺) after odor stimulation is significantly higher in the KO RUN mice with respect to the WT and KO NO RUN mice (KO RUN vs KO NO RUN, genotype × exercise interaction, $F_{(1,58)}=3.69$, $p<0.05$, followed by the analysis of simple effect, $***p<0.001$); KO RUN vs WT NO RUN, genotype × exercise interaction, $F_{(1,58)}=3.69$, $p<0.05$, followed by analysis of simple effect, $***p<0.001$). **j** Histogram showing the large increase of BrdU⁺NeuN⁺c-fos⁺ cells in Btg1-null mice olfactory bulb after 12-days running (KO RUN vs KO NO RUN, genotype × exercise interaction, $F_{(1,58)}=8.989$, $p<0.01$, followed by the analysis of simple effect, $***p<0.001$, KO RUN vs WT NO RUN, genotype × exercise interaction $F_{(1,58)}=8.989$, $p<0.01$, followed by the analysis of simple effect, $*p<0.05$). Cell numbers are mean ± SEM of the analysis of at least three animals per condition. $*p<0.05$, $**p<0.01$ or $***p<0.001$; ANOVA test

dramatic decline of the KO RUN mice neurospheres volume when compared with KO ($p<0.01$, Fig. 6d, f) and WT ($p<0.001$, Fig. 6d, f) mice, indicating an inability of KO RUN stem cells to divide symmetrically and to self-renewal after long term in vitro culture. The in vitro data clearly suggested that: (a) exercise triggered a hyper-proliferation and expansion capacity in the neural stem cells isolated from SVZ of KO RUN mice, during the first passages in vitro; (b) with time, we observed a progressive loss of self-renewal capacity of KO run activated NSCs. This event suggested that NSCs activation after running in KO RUN mice is not strictly cell autonomous but might depend on specific events occurring in the subventricular neurogenic niche during running, such as increase in expression of neurotrophins (BDNF, IGF-1), angiogenic remodeling, or microglia activation.

Effect of physical activity on 15-month-old SVZ of BTG1 KO mice

Many recent observations have well established that aging represents one of the main factors negatively regulating adult neurogenesis both in the dentate gyrus and the SVZ and that this process is nearly irreversible. To dispel this dogma, we wished to evaluate whether 12 days of physical activity might trigger the activation and expansion of neural stem cell pools also in the aged Btg1 KO mice. To do this, 15-month-old mice of the different experimental conditions were sacrificed, and proliferation, differentiation, and percentage of stem cells recruitment were calculated. In addition, in this case, we did not detect any volumetric differences of SVZ among the different experimental conditions (Suppl. Figure 1B). First at all, we observed that in Btg1 WT and Btg1 KO mice, SVZ neurogenesis dropped to a similar level, in terms of NSCs recruitment (Fig. 7e), proliferation (Fig. 7b), NSCs size (Fig. 7c, d), and early differentiation (Fig. 7g, h), suggesting that the physiological depletion of neural stem and progenitor cells with age reached a plateau of low neurogenic rate in both Btg1 WT and Btg1 KO mice. In the Btg1 null mice, 12 days of voluntary running still induced a strong pro-neurogenic effect; indeed, we observed a striking increase of cell proliferation (Ki67⁺ cells) in the KO RUN SVZ with respect to the other experimental groups ($p<0.001$ vs all the groups, Fig. 7a, b), which is reflected in a significant rise in the NSCs pool (Nestin⁺Sox⁺ cells, $p<0.001$ vs all the groups, Fig. 7a, c) as well as in the fraction of proliferating NSCs (Ki67⁺Nestin⁺Sox2⁺ cells) when compared to WT NO RUN and KO NO RUN mice ($p<0.001$ vs all the groups, Fig. 7a, d). However, our data showed that in KO RUN mice, the strong expansion of the NSCs pool is not followed by an equally large increase in the type A



pool (DCX⁺ and Ki67⁺/DCX⁺ cells, Fig. 7f, g, h), whose values matched those observed in the WT NO RUN mice. Surprisingly, in WT RUN mice, there is a dramatic increase in the number of DCX⁺ cells when compared with their sedentary counterpart (Fig. 7g), which, however, is not associated with a concomitant increase of proliferation (Fig. 7h), which leads us to assume a

post-mitotic neuroblast accumulation, rather than an increase of SVZ neurogenesis. All together, these results clearly state, for the first time, that aged subventricular neural stem cells devoid of the proliferative inhibition exerted by the Btg1 gene still retain a high potential for recruitment/activation from quiescence, for self-renewal replication and proliferation, when stimulated by an external event, such as physical activity.

Fig. 6 Running triggers in vitro expansion of the stem cell pool when Btg1 is deleted. **a** Representative images of secondary neurospheres derived from 2-month-old Btg1 WT, Btg1 KO, and Btg1 KO RUN mice after 14 days in vitro, showing the large increase of number and size of neurospheres derived from KO RUN mice. *Scale bar* 115 μ m. **b** Number of clonal neurospheres derived from the subependyma of the lateral ventricle from the different experimental groups. Relative to the WT mice, neurospheres generated from KO mice largely decreased (genotype \times exercise interaction, $F_{(1,18)}=11.347$, $p<0.01$, followed by the analysis of simple effect $*p<0.05$). Running is able to totally revert this phenotype, by greatly increasing the neurosphere number with respect to the KO NO RUN (genotype \times exercise interaction, $F_{(1,18)}=11.347$, $p<0.01$, followed by the analysis of simple effect $**p<0.01$) and to the WT NO RUN mice (genotype \times exercise interaction, $F_{(1,18)}=11.347$, $p<0.01$, followed by the analysis of simple effect $*p<0.05$). **c** In the absence of Btg1, the volumes of secondary neurospheres were smaller in comparison with the wild-type neurospheres (genotype \times exercise interaction, $F_{(1,233)}=39.983$, $p<0.001$, followed by the analysis of simple effect $***p<0.001$). The absence of Btg1 coupled with 12 days of running induced a large enhancement of neurosphere volume not only with respect to the sedentary Btg1 KO mice (genotype \times exercise interaction, $F_{(1,233)}=39.983$, $p<0.001$, followed by the analysis of simple effect $***p<0.001$) but also in comparison with WT NO RUN mice (genotype \times exercise interaction, $F_{(1,233)}=39.983$, $p<0.001$, followed by the analysis of simple effect $***p<0.001$). **d** Representative images of neurospheres after 35 days in vitro showing the strong diminution of size of the neurospheres derived from KO RUN mice. *Scale bar* 115 μ m. **e** Growth curve displaying the amplification of 8000 cells derived from secondary neurospheres plated at t_0 from P60 mice. The amplification of KO RUN cells is greatly reduced in the long term when compared with the other experimental conditions. **f** Graph showing the large decrease of the size of neurospheres derived from KO RUN mice in comparison with KO NO RUN (genotype \times exercise interaction, $F_{(1,144)}=13.384$, $p<0.001$, followed by the analysis of simple effect $**p<0.01$) and with WT NO RUN mice (genotype \times exercise interaction, $F_{(1,144)}=13.384$, $p<0.001$, followed by the analysis of simple effect $***p<0.001$). Neurosphere analysis are expressed as mean \pm SEM of the study of at least three animals per conditions. $*p<0.05$, $**p<0.01$ or $***p<0.001$; ANOVA test

Discussion

Rescue by physical exercise of SVZ cells with defective neurogenesis through cell cycle acceleration

Voluntary physical activity is one of the most potent inducers of adult neurogenesis (van Praag et al. 1999; Olson et al. 2006; Fabel and Kempermann 2008). However, the increase of the proliferation of neural progenitor cells is region-specific, since it occurs exclusively in the hippocampus, while no enhancement of neurogenesis is exerted by running in the SVZ (Brown et al. 2003). Nevertheless, a very recent work has emphasized a pro-neurogenic role of running in rats with a decreased subventricular neurogenesis induced by chronic infusion of corticosterone (Lee et al. 2016).

In this report, we observe a specific increase of neurogenesis elicited by running in the SVZ of Btg1 knockout

mice. In fact, the number of stem cells (B cells) and neuroblasts (C cells) in Btg1 knockout SVZ mice after running increases significantly above control (i.e., not running WT), while in WT mice, no change in B or A cells is effected by running, as expected. Moreover, as we have previously shown, in adult Btg1 knockout mice, the number of SVZ stem and neuroblast cells before running is significantly lower than in WT, indicating that the condition existing before application of the neurogenic stimulus is of reduced proliferative capability (Farioli-Vecchioli et al. 2014). Such a proliferative decrease follows after a period of hyperproliferation occurring early after birth in Btg1 knockout mice—consistent with the fact that Btg1 is a strong inhibitor of proliferation—and is probably the consequence of a compensatory increase of p21 levels (Farioli-Vecchioli et al. 2012, and data not shown).

The running-dependent increase in the number of Btg1-null stem cells (B cells) is maximally evident when these are identified as positive either to GFAP or to nestin and Sox2, with an increment of the total number of stem cells up to 50% and of proliferating stem cells of about 75%. Such an increase appears to depend on a progressive recruitment into the cell cycle, with an enhanced exit of Btg1 knockout stem cells from quiescence, in which the unstimulated Btg1 knockout SVZ stem cells preferentially remain. In fact, a depth analysis of the cell cycle profile shows that in both stem and neuroblast SVZ cells of Btg1 knockout mice not submitted to running, a major increase of the S-phase length occurs, accompanied by increased entry in quiescence, relative to wild-type either submitted or not to running. This cell cycle lengthening is evidently the counterpart of the reduced proliferative capability observed in SVZ cells of Btg1 knockout mice, mentioned above. Interestingly, normal aging mice also show increased entry into quiescence of SVZ progenitors (Luo et al. 2006), as occurs in Btg1 knockout mice, thus implying that this model reproduces aspects of the process of aging. Notably, after prolonged physical exercise, through a protocol of 12 days of voluntary running, the increase of the S-phase length in Btg1 knockout stem and neuroblast cells is fully reversed to control level (i.e., of wild-type mice submitted to exercise). This indicates that the SVZ stem cells lacking Btg1, despite the loss of their proliferative capability, and a lengthened cell cycle with a prevailing quiescent mode, can, nevertheless, be fully reactivated to control level by a neurogenic stimulus, such as running.

These findings obtained in Btg1 knockout SVZ are similar to that observed in the dentate gyrus, where 12 days of physical exercise increase neurogenesis above control, shortening the cell cycle length (Farioli-Vecchioli et al. 2012). This is the first study which analyzes the effect exerted by running on the cell cycle in wild-type SVZ stem and progenitor cells. Our data clearly state that

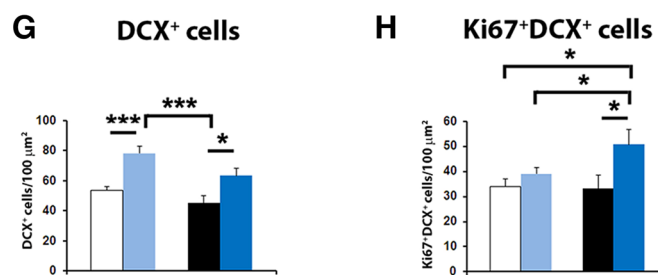
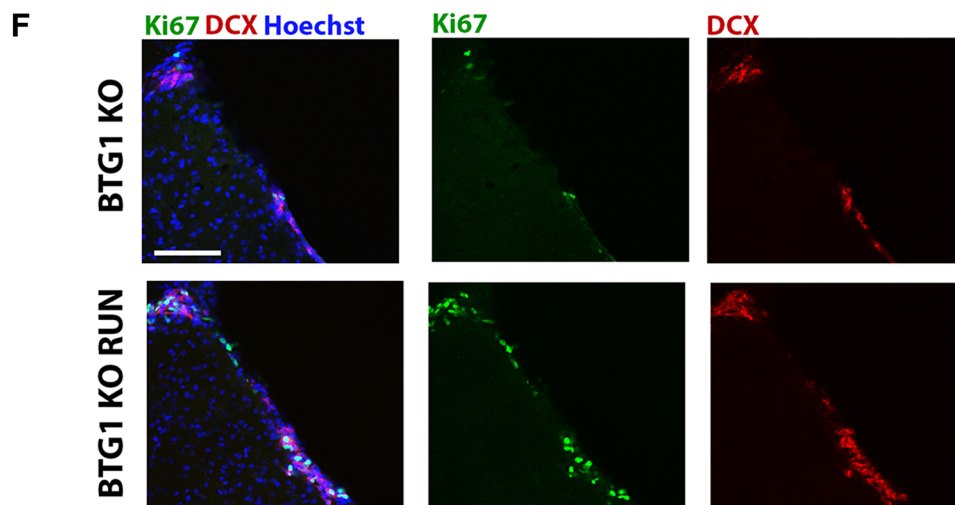
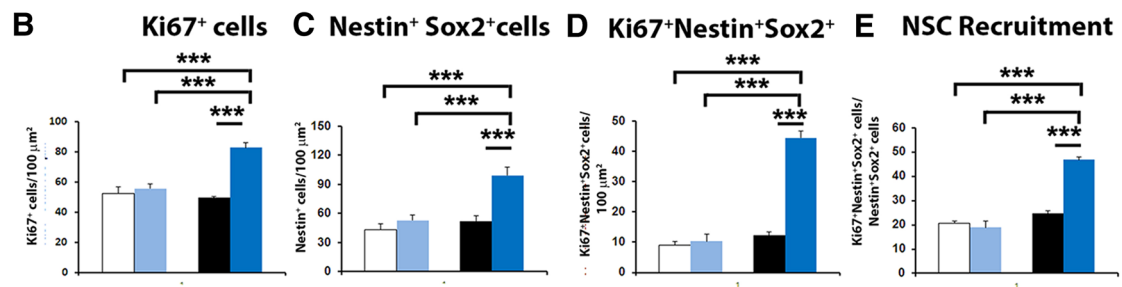
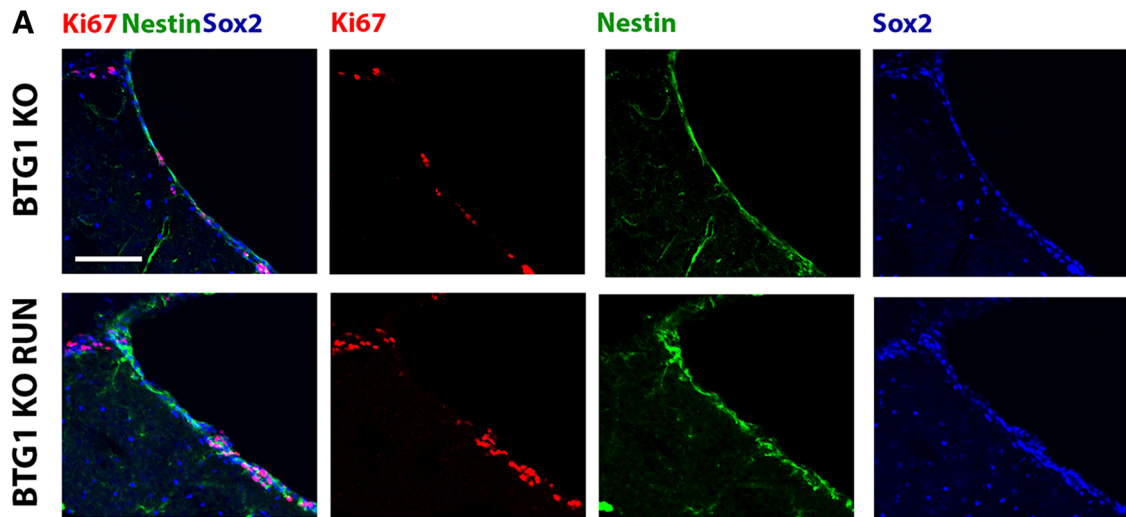


Fig. 7 Effects of running on SVZ neurogenesis of 15-month-old mice. **a** Representative fluorescence images of SVZ coronal sections of Ki67⁺/Nestin⁺/Sox2⁺ triple labeling, in *red*, *green*, and *blue*, respectively, showing the large increase of Type B NSCs in the 15-month old KO RUN with respect to the KO NO RUN mice. Scale bar 100 μm. **b** Running induces a strong increase of total cell proliferation with respect to the other experimental groups (KO RUN vs KO NO RUN genotype × exercise interaction, $F_{(1,62)}=22.724$, $p<0.001$ followed by the analysis of simple effect, $***p<0.001$; KO RUN vs WT NO RUN genotype × exercise interaction, $F_{(1,62)}=22.724$, $p<0.001$ followed by the analysis of simple effect, $***p<0.001$). **c, d** In the 15-month-old KO mice, 12 days of running results in a larger increase of type B cells (identified with Nestin and Sox2 markers) and of proliferating type B (expressing the Ki67, Nestin and Sox2 markers) cells in comparison with KO NO RUN and WT NO RUN mice (Nestin⁺/Sox2⁺ cells: KO RUN vs KO NO RUN genotype × exercise interaction, $F_{(1,31)}=7.839$, $p<0.01$ followed by the analysis of simple effect, $***p<0.001$; KO RUN vs WT NO RUN genotype × exercise interaction, $F_{(1,31)}=7.839$, $p<0.01$ followed by the analysis of simple effect, $***p<0.001$. Ki67⁺/Nestin⁺/Sox2⁺ cells: KO RUN vs KO NO RUN genotype × exercise interaction, $F_{(1,31)}=54.328$, $p<0.001$ followed by the analysis of simple effect, $***p<0.001$; KO RUN vs WT NO RUN genotype × exercise interaction, $F_{(1,31)}=54.328$, $p<0.001$ followed by analysis of simple effect, $***p<0.001$). **e** Histogram showing that the percentage of type B cells recruited from the quiescent state (ratio between Ki67⁺/Nestin⁺/Sox2⁺ and total Nestin⁺/Sox2⁺ cells) increased in aged KO RUN mice in comparison to KO NO RUN and WT NO RUN mice (genotype × exercise interaction, $F_{(1,31)}=15.547$, $p<0.001$, followed by the analysis of simple effect, $**p<0.001$; genotype × exercise interaction, $F_{(1,31)}=15.547$, $p<0.001$, followed by analysis of simple effect, $***p<0.001$, respectively). **f** Representing the increase of type A (DCX⁺ cells, *red*) and proliferating type A neuroblast (Ki67⁺DCX⁺ cells, *green* and *red*, respectively) in the aged KO RUN mice when compared with their sedentary counterparts. **g, h** Graphs illustrating the enhanced number of type A (DCX⁺ cells) and proliferating type A cells (Ki67⁺/DCX⁺) with respect to the KO NO RUN mice (DCX cells: treatment effect, $F_{(1,27)}=16.572$, $p<0.001$, followed by the analysis of simple effect $p<0.05$. Ki67⁺/DCX⁺ cells: treatment effect, $F_{(1,27)}=16.572$, $p<0.001$, followed by analysis of simple effect $*p<0.05$). Note the large increase of DCX⁺ cells in the aged WT RUN mice compared to their sedentary littermates (WT vs WT RUN: treatment effect, $F_{(1,27)}=16.572$, $p<0.001$, followed by the analysis of simple effect $p<***0.01$). Cell numbers are mean ± SEM of the analysis of at least three animals per conditions. $*p<0.05$, $**p<0.01$ or $***p<0.001$; ANOVA test

physical exercise is not able to alter the cell cycle kinetics in the physiological conditions, suggesting that the effect observed in Btg1 knockout mice is specific.

Remarkably, a decrease of the cell cycle length of Btg1 knockout stem/neuroblast cells is detectable also after a shorter period of running (5 days). This fact suggests that the change in cell cycle length, being quite early, may be a primary factor in the process of stem cell reactivation enacted by running in Btg1 knockout SVZ.

In fact, physical exercise rapidly induces a large number of processes, such as vasculogenesis and myogenesis, leading to a greater local availability for stem cells of peripheral factors, such as serotonin, FGF-2, IGF-1, VEGF, β-endorphin, and adiponectin, known for their stimulatory

effects on hippocampal proliferation (Bolin and Lucassen 2015). We cannot exclude that each of these events may also play a causal and/or synergistic role in the acceleration of the cell cycle observed in running mice lacking Btg1. Certainly, however, the running process is, as a whole, the primary event that reveals how the reduced proliferative capability of Btg1 knockout SVZ stem cells is an only apparent or transient condition, since it can be reversed. More remarkably, it shows a general property of SVZ stem cells not evidenced so far, i.e., that these are endowed with a residual proliferative capability which can be mobilized in case of need, through a cell cycle acceleration.

It is worth noting that the Kempermann's group has recently shown how a running schedule of 5 days did not change the temporal parameters of the cell cycle in dentate gyrus progenitor cells (Fischer et al. 2014). Moreover, since we have observed after 12 days of running an acceleration of the cell cycle (Farioli-Vecchioli et al. 2014), he suggested that running is not the primary causal event that modifies the cell cycle length. Our present data in SVZ seem to contradict this assumption. At any rate, it seems to us that the key point emerging from these data is the hidden ability of SVZ and dentate gyrus stem cells to recover from a state of reduced proliferation, after a neurogenic stimulus, also by modifying their cell cycle parameters.

In this context, it is possible that the acceleration of the cell cycle occurring after several days of running may act as a stabilizing factor for the increased expansion of the stem/progenitor cells in Btg1-null SVZ as well as dentate gyrus (see also Farioli-Vecchioli and Tirone 2015).

A recent study stated that in the dentate gyrus, a reliable increase in LTP was only observed after 56 days of running, suggesting that long-term exercise is needed to enhance synaptic plasticity in the hippocampus (Patten et al. 2013). Regarding the effect of the long-term run on subventricular neurogenesis, there are no currently available data and our study was limited to analyzing the pro-neurogenic effect of 12 days of running to compare the results with those obtained previously in the dentate gyrus of mice Btg1. Thus, we cannot rule out that long-term running might exert an even greater effect.

Remarkably, newborn neurons in Btg1 knockout mice migrate faster, not only in vivo, out of the SVZ to the olfactory bulb, but also in vitro. A reason for this may be that Btg1 knockout SVZ stem and neuroblast cells tend to exit from the cycle and consequently they begin to differentiate and migrate earlier. Indeed, a decrease of the rate of terminal differentiation (i.e., the ratio of BrdU+ NeuN+ cells to the total BrdU+ cells) was observed in Btg1 knockout neurons migrated to the olfactory bulb. Moreover, voluntary exercise, which restores a normal exit from the cell cycle, also re-establishes the normal rates of migration and differentiation. All this may suggest that the primary

signal triggering neuroblast migration is the exit from the cell cycle, rather than the differentiation. This excess of migration to the olfactory bulb of new Btg1 knockout neurons and the corresponding rescue exerted by running are observed also *in vitro* at the cellular level, thus indicating that the effect of running on migration is cell-intrinsic. This is also consistent with the possibility that the rescue to a normal cell cycle length exerted in Btg1 KO SVZ by running, being a cellular event, is the mechanism underlying the rescue of the defective migration and differentiation of the Btg1 knockout neuroblasts.

Furthermore, ablation of Btg1 did not interfere with the intrinsic ability of differentiated neurons in the olfactory bulb to be recruited in olfactory circuits, since the total c-fos+ neurons did not change. Remarkably, however, the Btg1 knockout neurons resulted after running more recruitable than wild-type neurons. A possibility that would account for such an effect may be that running, by accelerating the timing of differentiation in Btg1 knockout neuroblasts, may either induce a higher excitability, or, more probably, increase the fraction of differentiated neurons ready to be activated. This may be facilitated also by the fact that running is a stimulus strong enough to induce a large increase of the activation and expansion of the Btg1 knockout neural stem and progenitor cells, as we have seen in the pool of neurosphere culture. However, a limitation of this study is that control mice did not receive blocked wheels in the cages, since wheels could still represent an important pro-neurogenic stimulus, by providing the animals with an enriched environment in comparison with the empty cage. Ongoing studies specifically aim to fill this experimental constraint.

Possible mechanisms for the rescue of proliferation-defective SVZ stem cells

An interesting aspect emerging is that stem cells in Btg1 knockout aged mice after running show a greater expansion than occurs in WT, suggesting that the deprivation of Btg1 endows stem cells with a permanent greater proliferative capacity. However, Btg1 knockout SVZ neural stem cells cultivated *in vitro*, after an initial expansion triggered by running, undergo a loss of their proliferative potential. In this context, numerous studies clearly indicate that the proliferation of neural stem cells in the adult neurogenic niches is subjected to a fine-tuned regulation by numerous factors present in the niche, such as glucocorticoids, sex hormones, growth factors, neurotrophins, excitatory neurotransmission (Zhu et al. 2003; Gomez-Pinilla et al. 2008), angiogenic remodeling, or microglia activation (Platel and Bordey 2016), that orchestrate the recruitment and the proliferative kinetic of newborn neurons. This may imply that the greater proliferative

capability induced by running in Btg1 knockout stem cells either requires that the neurogenic stimulus be applied continuously or that, *in vitro*, some synergic factor correlated to running (see above) is missing, such as, for instance, Growth Hormone, neurotrophins (BDNF) or IGF-1 (Blackmore et al. 2012; Berchtold et al. 2005; Gomez-Pinilla et al. 2008).

The dual effect observed *in vivo* in adult Btg1 knockout DG and SVZ—i.e., decreased neurogenesis before the running stimulus and enhanced neurogenesis after—may involve, besides the peripheral factors cited (IGF-1 etc.), also p21 or cyclin D1. In fact, as mentioned above, p21 expression increases in the adult DG after Btg1 knockout (Farioli-Vecchioli et al. 2012), and such increase may be the cause for the lengthening of the S-phase in the mutant DG and, presumably, in the SVZ. Notably, p21 knockout elicits a response on neurogenesis similar to that of Btg1, since its ablation leads in the long term to a decrease of neurogenesis (Kippin et al. 2005). We can speculate that the p21 levels or function may be inhibited by physical exercise in the SVZ of Btg1 knockout mice. An opposite pattern of regulation in Btg1 knockout SVZ after running may occur for cyclin D1, which we have recently demonstrated to be selectively inhibited by Btg1 (in cerebellum precursor cells and in fibroblasts; Ceccarelli et al. 2015). Whereas the cyclin-dependent kinase inhibitor p16 is a possible candidate accounting for the lack of difference in neurogenesis between aging wild-type and Btg1 knockout SVZ, since p16 increases during aging and its deletion increases the self-renewal of SVZ stem cells (Molofsky et al. 2005) as well as the generation of new neurons in old mice (15–19 months; Molofsky et al. 2006).

Conclusions

Therefore, as a whole, our data in the SVZ show how SVZ neurogenesis can be modulated by cell cycle kinetics. Indeed, they point to the fact that in particular conditions, such as in the absence of a proliferative inhibitor (Btg1) and in the presence of a powerful neurogenic stimulus, such as voluntary running, the proliferative capability of stem cells turns out to be more plastic than hitherto supposed, and to be correlated to cell cycle changes. Since the neurons produced by SVZ stem cells can be redirected to the damaged region during neurodegenerative events, such as stroke (Christie and Turnley 2013), our findings may open new possibilities for therapeutic approaches.

Acknowledgements This work was supported by CNR projects DSB.AD004.093 to Felice Tirone.

Compliance with ethical standards

Conflict of interest The authors indicate no potential conflict of interests.

References

- Alvarez-Buylla A, Kohwi M, Nguyen TM, Merkle FT (2008) The heterogeneity of adult neural stem cells and the emerging complexity of their niche. *Cold Spring Harb Symp Quant Biol* 73:357–365
- American College of Sports Medicine; Chodzko-Zajko WJ, Proctor DN, Fiatarone Singh MA, Minson CT, Nigg CR, Salem GJ, Skinner JS American College of Sports Medicine position stand (2009) Exercise and physical activity for older adults. *Med Sci Sports Exerc* 41(7):1510–1530
- Bednarczyk MR, Aumont A, Décary S, Bergeron R, Fernandes KJ (2009) Prolonged voluntary wheel-running stimulates neural precursors in the hippocampus and forebrain of adult CD1 mice. *Hippocampus* 19(10):913–927
- Berchtold NC, Chinn G, Chou M, Kessler JP, Cotman CW (2005) Exercise primes a molecular memory for brain-derived neurotrophic factor protein induction in the rat hippocampus. *Neuroscience* 133(3):853–861
- Beukelaers P, Vanderbosch R, Caron N, Nguyen L, Belachew S, Moonen G, Kiyokawa H, Barbacid M, Santamaria D, Malgrange B (2011) Cdk6-dependent regulation of G1 length controls adult neurogenesis. *Stem Cells* 29:713–724
- Blackmore DG, Reynolds BA, Golmohammadi MG, Large B, Aguilar RM, Haro L, Waters MJ, Rietze RL (2012) Growth hormone responsive neural precursor cells reside within the adult mammalian brain. *Sci Rep* 2:250
- Bolijn S, Lucassen PJ (2015) How the body talks to the brain; peripheral mediators of physical activity-induced proliferation in the adult hippocampus. *Brain Plastic* 1(1):15–27
- Brandt MD, Hübner M, Storch A (2012) Brief report: adult hippocampal precursor cells shorten S-phase and total cell cycle length during neuronal differentiation. *Stem Cells* 30(12):2843–2847
- Brown J, Cooper-Kuhn CM, Kempermann G, Van Praag H, Winkler J, Gage FH, Kuhn HG (2003) Enriched environment and physical activity stimulate hippocampal but not olfactory bulb neurogenesis. *Eur J Neurosci* 17(10):2042–2046
- Cai L, Hayes NL, Nowakowski RS (1997) Local homogeneity of cell cycle length in developing mouse cortex. *J Neurosci* 17(6):2079–2087
- Carleton A, Petreanu LT, Lansford R, Alvarez-Buylla A, Lledo PM (2003) Becoming a new neuron in the adult olfactory bulb. *Nat Neurosci* 6(5):507–518
- Ceccarelli M, Micheli L, D'Andrea G, De Bardi M, Scheijen B, Ciotti M, Leonardi L, Luvisetto S, Tirone F (2015) Altered cerebellum development and impaired motor coordination in mice lacking the Btg1 gene: involvement of cyclin D1. *Dev Biol* 408(1):109–125
- Christie KJ, Turnley AM (2013) Regulation of endogenous neural stem/progenitor cells for neural repair-factors that promote neurogenesis and gliogenesis in the normal and damaged brain. *Front Cell Neurosci* 6:70
- Colak D, Mori T, Brill MS, Pfeifer A, Falk S, Deng C, Monteiro R, Mummery C, Sommer L, Götz M (2008) Adult neurogenesis requires Smad4-mediated bone morphogenetic protein signaling in stem cells. *J Neurosci* 28(2):434–446
- Danzer SC (2012) Depression, stress, epilepsy and adult neurogenesis. *Exp Neurol* 233(1):22–32
- Dietrich MO, Andrews ZB, Horvath TL (2008) Exercise-induced synaptogenesis in the hippocampus is dependent on UCP2-regulated mitochondrial adaptation. *J Neurosci* 28(42):10766–10771
- Dimitrov EL, Tsuda MC, Cameron HA, Usdin TB (2014) Anxiety- and depression-like behavior and impaired neurogenesis evoked by peripheral neuropathy persist following resolution of prolonged tactile hypersensitivity. *J Neurosci* 34(37):12304–12312
- Doetsch F, Caillé I, Lim DA, García-Verdugo JM, Alvarez-Buylla A (1999) Subventricular zone astrocytes are neural stem cells in the adult mammalian brain. *Cell* 97(6):703–716
- Fabel K, Kempermann G (2008) Physical activity and the regulation of neurogenesis in the adult and aging brain. *Neuromol Med* 10(2):59–66
- Farioli-Vecchioli S, Tirone F (2015) Control of cell cycle in adult neurogenesis and its relation with physical exercise. *Brain Plastic* 1:41–54
- Farioli-Vecchioli S, Micheli L, Sarauili D, Ceccarelli M, Cannas S, Scardigli R, Leonardi L, Cinà I, Costanzi M, Ciotti MT, Moreira P, Rouault JP, Cestari V, Tirone F (2012) Btg1 is required to maintain the pool of stem and progenitor cells of the dentate gyrus and subventricular zone. *Front Neurosci* 6:124
- Farioli-Vecchioli S, Mattera A, Micheli L, Ceccarelli M, Leonardi L, Sarauili D, Costanzi M, Cestari V, Rouault JP, Tirone F (2014) Running rescues defective adult neurogenesis by shortening the length of the cell cycle of neural stem and progenitor cells. *Stem Cells* 32(7):1968–1982
- Fischer TJ, Walker TL, Overall RW, Brandt MD, Kempermann G (2014) Acute effects of wheel running on adult hippocampal precursor cells in mice are not caused by changes in cell cycle length or S phase length. *Front Neurosci* 8:314
- Gomez-Pinilla F, Vaynman S, Ying Z (2008) Brain-derived neurotrophic factor functions as a metabotrophin to mediate the effects of exercise on cognition. *Eur J Neurosci* 28(11):2278–2287
- Imura T, Kornblum HI, Sofroniew MV (2003) The predominant neural stem cell isolated from postnatal and adult forebrain but not early embryonic forebrain expresses GFAP. *J Neurosci* 23(7):2824–2832
- Intlekofer KA, Berchtold NC, Malvaez M, Carlos AJ, McQuown SC, Cunningham MJ, Wood MA, Cotman CW (2013) Exercise and sodium butyrate transform a subthreshold learning event into long-term memory via a brain-derived neurotrophic factor-dependent mechanism. *Neuropsychopharmacology* 38(10):2027–2034
- Itoh T, Imano M, Nishida S, Tsubaki M, Hashimoto S, Ito A, Satou T (2011) Exercise increases neural stem cell proliferation surrounding the area of damage following rat traumatic brain injury. *J Neural Transm (Vienna)* 118(2):193–202
- Kippin TE, Martens DJ, van der Kooy D (2005) p21 loss compromises the relative quiescence of forebrain stem cell proliferation leading to exhaustion of their proliferation capacity. *Genes Dev* 19(6):756–767
- Kohwi M, Osumi N, Rubenstein JL, Alvarez-Buylla A (2005) Pax6 is required for making specific subpopulations of granule and periglomerular neurons in the olfactory bulb. *J Neurosci* 25(30):6997–7003
- Kosaka K, Aika Y, Toida K, Heizmann CW, Hunziker W, Jacobowitz DM, Nagatsu I, Streit P, Visser TJ, Kosaka T (1995) Chemically defined neuron groups and their subpopulations in the glomerular layer of the rat main olfactory bulb. *Neurosci Res* 23(1):73–88
- Kronenberg G, Bick-Sander A, Bunk E, Wolf C, Ehninger D, Kempermann G (2006) Physical exercise prevents age-related decline in precursor cell activity in the mouse dentate gyrus. *Neurobiol Aging* 27(10):1505–1513
- Laywell ED, Rakic P, Kukekov VG, Holland EC, Steindler DA (2009) Identification of a multipotent astrocytic stem cell in

- the immature and adult mouse brain. *Proc Natl Acad Sci USA* 97(25):13883–13888
- Lee JC, Yau SY, Lee TM, Lau BW, So KF (2016) Voluntary wheel running reverses the decrease in subventricular zone neurogenesis caused by corticosterone. *Cell Transpl*. doi:10.3727/096368916X692195
- Lim DA, Alvarez-Buylla A (2016) The adult ventricular-subventricular zone (V-SVZ) and olfactory bulb (OB) neurogenesis. *Cold Spring Harb Perspect Biol* 8(5)
- Lin TW, Chen SJ, Huang TY, Chang CY, Chuang JI, Wu FS, Kuo YM, Jen CJ (2012) Different types of exercise induce differential effects on neuronal adaptations and memory performance. *Neurobiol Learn Mem* 97(1):140–147
- Luo J, Daniels SB, Lenington JB, Notti RQ, Conover JC (2006) The aging neurogenic subventricular zone. *Aging Cell* 5(2):139–152
- Molofsky AV, He S, Bydon M, Morrison SJ, Pardal R (2005) Bmi-1 promotes neural stem cell self-renewal and neural development but not mouse growth and survival by repressing the p16Ink4a and p19Arf senescence pathways. *Genes Dev* 19(12):1432–1437
- Molofsky AV, Slutsky SG, Joseph NM, He S, Pardal R, Krishnamurthy J, Sharpless NE, Morrison SJ (2006) Increasing p16INK4a expression decreases forebrain progenitors and neurogenesis during ageing. *Nature* 443(7110):448–452
- Niwa A, Nishibori M, Hamasaki S, Kobori T, Liu K, Wake H, Mori S, Yoshino T, Takahashi H (2016) Voluntary exercise induces neurogenesis in the hypothalamus and ependymal lining of the third ventricle. *Brain Struct Funct* 221(3):1653–1666
- Olson AK, Eadie BD, Ernst C, Christie BR (2006) Environmental enrichment and voluntary exercise massively increase neurogenesis in the adult hippocampus via dissociable pathways. *Hippocampus* 16(3):250–260
- Overall RW, Walker TL, Fischer TJ, Brandt MD, Kempermann G (2016) Different mechanisms must be considered to explain the increase in hippocampal neural precursor cell proliferation by physical activity. *Front Neurosci* 10:362
- Paillard T, Rolland Y, de Souto Barreto P (2015) Protective effects of physical exercise in Alzheimer's disease and Parkinson's disease: a narrative review *J Clin Neurol* 11(3):212–219
- Patten AR, Sickmann H, Hryciw BN, Kucharsky T, Parton R, Kernick A, Christie BR (2013) Long-term exercise is needed to enhance synaptic plasticity in the hippocampus. *Learn Mem* 20(11):642–647
- Platel JC, Bordey A (2016) The multifaceted subventricular zone astrocyte: From a metabolic and pro-neurogenic role to acting as a neural stem cell. *Neuroscience* 323:20–28
- Ruan L, Lau BW, Wang J, Huang L, Zhuge Q, Wang B, Jin K, So KF (2014) Neurogenesis in neurological and psychiatric diseases and brain injury: from bench to bedside. *Prog Neurobiol* 115:116–137
- Ryan SM, Kelly ÁM (2016) Exercise as a pro-cognitive. Pro-neurogenic anti-inflammatory intervention in transgenic mouse models of Alzheimer's disease. *Age Res Rev* 27:77–92
- Stranahan AM, Zhou Y, Martin B, Maudsley S (2009) Pharmacometrics of exercise: novel approaches for hippocampally-targeted neuroprotective agents. *Curr Med Chem* 16(35):4668–4678
- van Praag H (2008) Neurogenesis and exercise: past and future directions. *Neuromolecular Med* 10(2):128–140
- van Praag H, Christie BR, Sejnowski TJ, Gage FH (1999) Running enhances neurogenesis, learning, and long-term potentiation in mice. *Proc Natl Acad Sci USA* 96(23):13427–13431
- van Praag H, Shubert T, Zhao C, Gage FH (2005) Exercise enhances learning and hippocampal neurogenesis in aged mice. *J Neurosci* 25(38):8680–8685
- Wichterle H, Garcia-Verdugo JM, Alvarez-Buylla A (1997) Direct evidence for homotypic, glia-independent neuronal migration. *Neuron* 18(5):779–791
- Zhao C, Deng W, Gage FH (2008) Mechanisms and functional implications of adult neurogenesis. *Cell* 132(4):645–660
- Zhu Y, Jin K, Mao XO, Greenberg DA (2003) Vascular endothelial growth factor promotes proliferation of cortical neuron precursors by regulating E2F expression. *FASEB J* 17(2):186–193